UNSATURATED FLOW IN SWELLING AND NONSWELLING SOILS

BY

R. N. YONG AND H. Y. WONG

SOIL MECHANICS SERIES No. 33

NOVEMBER 1974

SOIL MECHANICS LABORATORY

McGILL UNIVERSITY

DEPARTMENT OF CIVIL ENGINEERING AND APPLIED MECHANICS

MONTREAL, CANADA

FOREWORD

THE study of unsaturated flow in soils has generally considered the situation where the boundaries of the soil material are confined to the extent that volume change is negligible. In addition, assumptions are made regarding negligible pore geometry changes and developed swelling forces.

The above constraints tend to be too restrictive at times as a general treatment of the problem of fluid flow in unsaturated soils. The following four papers consider the problem of fluid flow in both swelling and nonswelling soils where account is given to pore geometry changes, volume changes, and developed swelling forces in saturations where volume change is restricted.

THE four papers are reprints from journals and conferences, and are listed as follows:

1. "On the Physics of Unsaturated Flow in Expansive Soils", R. N. Yong. Proc., 3rd Int. Conf. on Expansive Soils, Haifa, Israel. 1973. Vol. 2.

2. "A Study of Swelling and Swelling Force during Unsaturated Flow in Expansive Soils", H. Y. Wong and R. N. Yong. Proc., 3rd Int. Conf. on Expansive Soils, Haifa, Israel. 1973. Vol. 1.

3. "Engineering Problems in Unsaturated Soils", H. Y. Wong and R. N. Yong. Civil Engineering and Public Works Review (Gt. Britain). September 1973.

4. "Impedance Effects on Unsaturated Flow in a Nonswelling Soil", H. Y. Wong and R. N. Yong. J., Soil Mechanics and Foundations Div., Proc., American Society of Civil Engineers, V.98:SM8, August 1972.

Soil Mechanics Research Laboratory
November 1974.

Proc., 3rd Int. Conf. on Expansive Soils, Haifa, Israel. 1973. Vol. 2.

ON THE PHYSICS OF UNSATURATED FLOW IN EXPANSIVE SOILS

R. N. YONG,
William Scott Professor of Civil Engineering and Applied Mechanics
McGill University, Montreal, Canada

SYNOPSIS Unsaturated fluid flow in porous semi-rigid bodies [e.g. non-swelling clays] can be described in a fashion similar to heat flow analysis. However, when volume change occurs during flow, continuity relationships must be suitably modified. In addition, the various material coefficients relating unsaturated flow characteristics to material properties are seen to be directly affected. Thus, for a proper prediction of unsaturated flow in expansive soils where volume change is expected to occur, a proper accounting of the physics of the problem is necessary in order that correspondence between the physical and analytical models be achieved.

INTRODUCTION

The description of unsaturated fluid flow in soils can be simply categorized and analyzed according to two general types and conditions. These describe the different phenomena involving soil fabric and structure change occurring during the flow process and development of associated internal gradients. Of particular interest here is the phenomenon of volume change during and as a consequence of unsaturated flow. This situation is typical of fluid flow in unsaturated expansive soils in the unconstrained state. In general, however, we can class the two types of flow as:

Type 1 - Unsaturated flow in low swelling or non-swelling soils where no change in soil fabric occurs, i.e. little or no change in pore geometry and porosity during and as a result of infiltration,

Type 2 - Unsaturated flow in expansive soils where swelling pressures develop in confined flow, or a complete change in fabric and structure occurs in unconstrained flow, i.e. a change in pore geometry as well as in porosity and forces of interaction.

Type 1 flow describes the situation for a low swelling or non-swelling soil with negligible changes in pore geometry and with the physical boundaries perfectly confined. This case fits the situation encountered in cemented or highly compact material and other low swelling soils with no significant development of swelling pressures.

In Type 2, we include unsaturated fluid flow in a swelling clay where either confined or unconfined swelling is allowed to occur. Changes in forces of interaction, or in pore volume and overall soil volume would obviously alter fluid transmission characteristics. This study directs its attention to the description of the physics of unsaturated flow in the type 2 case [expansive soils] - with initial description of the general type 1 situation shown for background development. The intent is to provide correspondence between both physical and analytical models for admissible and viable predictions of unsaturated flow in expansive soils.

GENERAL UNSATURATED FLOW EQUATIONS FOR LOW SWELLING SOILS

The general treatment for unsaturated fluid flow in soils satisfying the physical condition of little or no volume change during and as a result of flow leads to the development of a working equation analogous to the heat flow equation. The analytical model invoked presumes that Darcy's law is valid for unsaturated flow. Thus, if we replace the hydraulic gradient grad h with the soil water potential gradient grad ψ, the Darcy equation may be written as:

$$\vec{v} = -k \text{ grad } \psi \qquad (1)$$

where

$\vec{v}$ = vector flow velocity

$$\text{grad } \psi = \left(\frac{\partial}{\partial x}\vec{i} + \frac{\partial}{\partial y}\vec{j} + \frac{\partial}{\partial z}\vec{k}\right)\psi$$

where the negative sign in equation (1) accounts for the fact that fluid flow is in the direction of decreasing potential. The equation of continuity, which satisfies the conservation of mass shows that the flow of water into or out of a unit of soil equals the rate of change in water content. Implicitly, this indicates that the system is preserved, and that no volume change occurs. Thus:

$$\text{div } \vec{v} = -\frac{\partial \theta}{\partial t} \quad \dots \quad (2)$$

where

$$\text{div } \vec{v} = \left(\frac{\partial}{\partial x}\vec{i} + \frac{\partial}{\partial y}\vec{j} + \frac{\partial}{\partial z}\vec{k}\right)\cdot v$$

θ = volumetric water content of the soil.

This situation is not likely to be true in expansive soils where semi-constrained or unrestrained swelling is allowed to occur during infiltration. For the low swelling soil however, one proceeds to obtain the three dimensional diffusion equation by substituting equation (2) into equation (1). Thus:

$$\frac{\partial \theta}{\partial t} = \text{div } (k \text{ grad } \psi) \quad \dots \quad (3)$$

Defining ψ as the sum of ψ_p, ψ_π and ψ_m, the pressure, osmotic and matric potential respectively, we note that for low swelling or inactive soils, ψ_π and ψ_m may be assumed to be small and insignificant. This renders ψ_p as the component potential of primary interest and concern. In the general treatment of the problem, the one dimensional case is considered. The usual procedure employed assumes that ψ_p is a unique function of θ. Thus, equation (3) is reduced to:

$$\frac{\partial \theta}{\partial t} = \frac{\partial}{\partial x}\left(D(\theta)\frac{\partial \theta}{\partial x}\right) \quad \dots \quad (4)$$

where x is the horizontal coordinate axis and $D(\theta)$ = diffusivity or diffusion coefficient of water = $k(\theta)\frac{\partial \psi_p}{\partial \theta}$. Equation (4) is seen to be analogous to the equation used to describe one dimensional thermal diffusion of heat.

Graphically [experimental] aided solutions to equation (4) can be obtained in the form of values of θ versus x or z at the different times, t. [*Figure 1*]. Values of k as a function of θ are determined experimentally, or may in some cases be calculated. Values of $\frac{\partial \psi_p}{\partial \theta}$ *are measured* from the slope of the soil water potential versus water content curve for the soil.

The diffusion equation [i.e. equation (4)] is solved analytically within the framework defined by the boundary conditions relevant to the problem under consideration. It is observed that the admissibility of the diffusion equation for solution of the problem at hand depends upon the conditions leading to its formulation, i.e. the assumption that [1] Darcy's law is valid, and [2] $D = D(\theta)$, which results from the definition:

$$D = k(\theta)\frac{\partial \psi}{\partial \theta} = 1(\theta)\frac{\partial \psi_p}{\partial \theta} \quad \dots \quad (5)$$

If swelling of the soil sample occurs during and as a result of infiltration, the specialised form of the continuity equation given in equation (2) which requires fluid incompressibility and no volume change, is no longer valid. The rate of movement of water relative to a fixed coordinate system is not similar to that with respect to the soil particles in view of soil expansion. Thus the diffusion equation shown as equation (4) utilizing this continuity condition is strictly not admissible. By resorting to a *similarity solution technique*, e.g. utilizing the Boltzman transform:

$$\lambda = \frac{x}{\sqrt{t}} = \lambda(\theta) \quad \dots \quad (6)$$

it becomes possible to reduce equation (4) for description of infiltration into low swelling soils to an ordinary differential equation:

$$\frac{\lambda}{2}\frac{d\theta}{d\lambda} = \frac{d}{d\lambda}\left(D\frac{d\theta}{d\lambda}\right) \quad \dots \quad (7)$$

When the physical requirements of infiltration correspond to those imposed by utilization of the similarity solution, i.e. actual physical linearity is obtained between x and $\sqrt{t}$ as demanded by the Boltzmann transform, solution of equation (7) will provide for adequate description of unsaturated flow into low swelling soils. Under the usual experimental situations, the physical constraints imposed provide for the following boundary conditions:

$t = 0$, $0 < x < \infty$ (thus $\lambda = \infty$), $\theta = \theta_i$

$t > 0$, $x = 0$ (thus $\lambda = 0$) $\theta = \theta_o$,

i.e. θ at $x = 0$

the total amount of water entering per unit area $(q_t)_o$ at the plane $x = 0$ can thus be obtained as:

$$(q_t)_o = t^{\frac{1}{2}}\int_{\theta_i}^{\theta_o} \lambda \, d\theta = \int_{\theta_i}^{\theta} x dx \quad \dots \quad (8)$$

The physical performance demonstrated by equation (8) may be seen in the three-dimensional representation of flow into an unsaturated soil [Figure 1] - depicting time, distance from source of water and volumetric moisture content. The wetting front profiles shown on the vertical plane projection in Figure 1 are characteristic for the situation of unsaturated flow with little or no volume change. The total quantity of water at any time [and thus at any position] will be indicated by the volume under the $\theta - x - \sqrt{t}$ surface shown in Figure 1. We note that projection onto the horizontal plane provides a linear relationship between x and $\sqrt{t}$ thus satisfying the assumption used in equation (6).

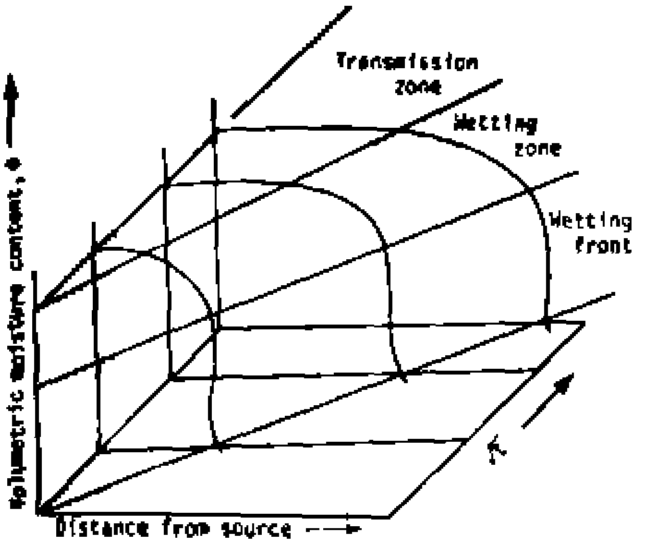

FIG.1: CHARACTERISTIC UNSATURATED FLOW BEHAVIOUR IN LITTLE OR NO VOLUME CHANGE SOILS. NOTE THE TYPICAL WET FRONT PROFILE AND LINEARITY OBTAINED IN THE $x - \sqrt{t}$ PLANE

VOLUME CHANGE CONSIDERATIONS IN UNSATURATED FLOW EQUATIONS

The curves shown in Figure 2 demonstrate physical $x - \sqrt{t}$ relationships for unsaturated flow into several kinds of soils and under specific conditions. Included is the constant porosity situation for a low swelling soil where linearity between x and $\sqrt{t}$ exists, which thus permits the application of the Boltzmann transform. This situation is represented by curve B. It is apparent that if curves A, C and D in Figure 2 are encountered, application of the Boltzmann transform as a similarity solution technique is no longer possible. It becomes necessary therefore to work with the generalized diffusion equation [equation 4].

An examination of the flow characteristics typifying curves A, C and D, shows that one of the primary reasons for departure from linearity in the $x - \sqrt{t}$ relationship is because of volume changes occurring during flow. This may be due [1] to a decrease in volume as in the case of low density soils which will collapse in the presence of increased water availability[curve A], or [2]

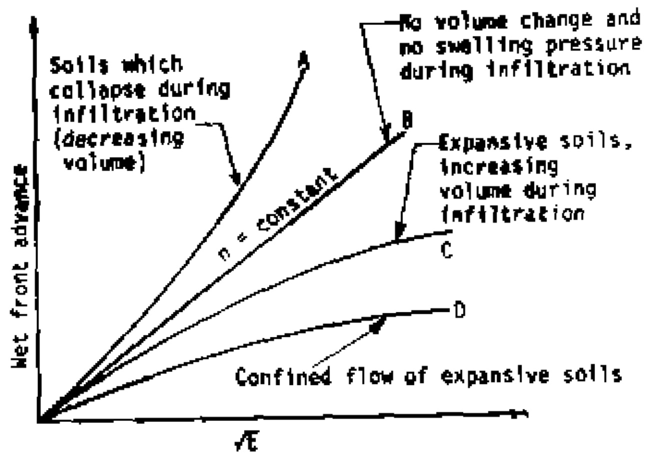

FIG.2: WET FRONT ADVANCE PROFILES SHOWING INFLUENCE OF VOLUME CHANGE AND SWELLING PRESSURE ON PROFILE DEVELOPMENT

to an increase in volume as in the case of swelling soils allowed to swell in the presence of available water [due to unsaturated flow]. This is represented by curve C. The situation represented by curve D is one of unsaturated flow in swelling soils where no volume change is allowed to occur. The presence of increased swelling pressures will result in alteration of flow characteristics.

To account for volume change of soil samples during infiltration, an approximate method would be to tie in the volumetric water content θ with porosity n and degree of saturation S. Thus, if we consider the horizontal infiltration case for illustrative purposes, and if V_x = velocity of flow in the x direction, one obtains:

$$\frac{\partial V_x}{\partial x} = -\frac{\partial}{\partial t}(nS)$$

$$= -\left[S\frac{\partial n}{\partial t} + n\frac{\partial S}{\partial t}\right] \quad \ldots \quad (9)$$

The diffusion equation for horizontal unsaturated flow now becomes:

$$S\frac{\partial n}{\partial t} + n\frac{\partial S}{\partial t} = \frac{\partial}{\partial x}\left(D\,\frac{\partial \theta}{\partial x}\right) \quad \ldots \quad (10)$$

Equation (10) is approximate in that the actual physics of flow which requires that D be suitably modified to account for the influence of volume change on D and also on k have not been incorporated in the analysis. For small changes in porosity n, it is expected that the approximate relationship will adequately describe the situation under consideration.

A simple accounting for D and $\frac{\partial\theta}{\partial x}$ in view of volume change can be achieved by introducing a change in the value of x which recognizes, in effect, a changing porosity. Thus, defining x' as:

$$x' = x + \frac{\delta n}{n} \quad .. \quad .. \quad .. \quad .. \quad .. \quad (11)$$

equation (10) can now be obtained as:

$$\theta \frac{\partial n}{\partial t} + n \frac{\partial S}{\partial t} = \frac{\partial}{\partial x}\left[D' \frac{\partial\theta'}{\partial x'}\right] \quad .. \quad .. \quad (12)$$

where θ' = volumetric water content in view of x' and D' = D(θ'), i.e. the diffusivity D' is a function of θ'.

In the treatment by Philip and Smiles (1969) the accounting for volume change is made by using a material coordinate system in the analytical formulation which renders it similar, in a sense, to the no-volume change analysis. Specifying the relation between material coordinate m and x as:

$$m = \int_{-\infty}^{x} \frac{dx}{1 + e} \quad .. \quad .. \quad .. \quad .. \quad (13)$$

where e = void ratio, the corresponding continuity condition is obtained as:

$$\frac{\partial}{\partial t}\left[\theta(1 + e)\right] = - \frac{\partial V_{ws}}{\partial m} \quad .. \quad .. \quad .. \quad (14)$$

where V_{ws} = velocity of water relative to moving soil particles.

The resultant diffusion equation obtained by Philip and Smiles thus becomes:

$$C \frac{\partial\theta}{\partial t} = \frac{\partial}{\partial m} (D_m \frac{\partial\theta}{\partial m}) \quad .. \quad .. \quad .. \quad .. \quad (15)$$

where

e and ψ are considered functions of θ only, and

$$C = 1 + e + \theta \frac{de}{d\theta}$$

$$D_m = (1 + e)^{-1} k \frac{d\psi}{d\theta}$$

The similarity transformation technique used previously can be used to relate m with $\sqrt{t}$ to provide:

$$\lambda' = \frac{m}{\sqrt{t}} \quad .. \quad .. \quad .. \quad .. \quad .. \quad (16)$$

Thus, so long as the requirements of this similarity transform are met [i.e. linearity] the solutions obtained in view of volume change will be correct. Thus equation (15) can now be reduced to an ordinary differential equation and solved subject to appropriate specification of boundary conditions.

A GENERALIZED UNSATURATED FLOW EQUATION

Consider an elemental soil volume of dimensions dx, dy and dz, with one dimensional unsaturated flow in the x-direction. Soil particle flow into and out of the elemental cube must satisfy conservation principles as follows:

$$\frac{\partial V_{sx}}{\partial x} = \frac{1}{1 - n} \frac{\partial n}{\partial t} \quad .. \quad .. \quad .. \quad .. \quad .. (17)$$

where V_{sx} = velocity of soil particles in the x direction. Since

$$\frac{1}{1 - n} \frac{\partial n}{\partial t} = \frac{\partial v}{\partial t} \quad .. \quad .. \quad .. \quad .. \quad (18)$$

where v = volumetric strain, one obtains:

$$\frac{\partial V_{sx}}{\partial x} = \frac{\partial v}{\partial t} \quad .. \quad .. \quad .. \quad .. \quad (19)$$

Decomposing the total fluid velocity into its two components:

[a] fluid flow relative to the moving soil particles, and

[b] soil particle flow contained in the fluid phase which will be in a position to move:

$$V_x = V_{wsx} + \theta V_{sx} \quad .. \quad .. \quad .. \quad (20)$$

where V_{wsx} = water movement relative to the moving soil particles.

One will obtain with equation (20) and the Darcian relationship, the following:

$$\frac{\partial V_x}{\partial x} = - \frac{\partial}{\partial x}\left[k \frac{\partial\psi}{\partial x}\right] + \theta \frac{\partial v}{\partial t} \quad .. \quad .. \quad (21)$$

Using the same assumptions for the diffusion coefficient D equation (21) now states that:

$$\frac{\partial V_x}{\partial x} = - \left[D \frac{\partial\theta}{\partial x}\right] + \theta \frac{\partial v}{\partial t} \quad .. \quad .. \quad .. \quad (22)$$

Using the continuity condition with attendant volume changes suitably accounted for, as:

$$\frac{\partial V_x}{\partial x} = - \frac{\partial\theta}{\partial t} \quad .. \quad .. \quad .. \quad .. \quad (23)$$

the resultant one dimensional horizontal diffusion equation which allows for volume change thus states that:

$$\frac{\partial\theta}{\partial t} = \frac{\partial}{\partial x}\left[D \frac{\partial\theta}{\partial x}\right] - \theta \frac{\partial v}{\partial t} \quad .. \quad .. \quad .. \quad (24)$$

If no volume change occurs during flow, $\frac{\partial v}{\partial t} = 0$, and equation (24) is reduced to the form shown in equation (4). A relationship similar to that shown by equation (24) can be obtained [with certain simplifying assumptions] from a more rigorous base, using the requirement that the flux of soil particles must satisfy [a] continuity, [b] Newton's law of motion, and [c] rheological equation of state. This approach has recently been used by Wong (1973). Considering the motion of soil particles in the volume changing soil during fluid flow as being slow, the acceleration considerations implicit in Newton's law of motion can be safely ignored in the analysis. The continuity relationship which satisfies conservation of mass can be written [in a fixed coordinate system] as:

$$\text{div}(\rho \vec{q}_s) + \frac{\partial \rho}{\partial t} = 0 \quad \ldots \quad (25)$$

where $\vec{q}_s$ = soil flux (vector)

ρ = bulk density = $\frac{G_s \rho_w}{1+e}$

ρ_w = density of water .. .. (26)

e = void ratio

G_s = specific gravity of solid particle

t = time

From equations (26) and (25)

$$\text{div}\,\vec{q}_s = \frac{1}{1+e}\frac{\partial e}{\partial t} + \frac{\vec{q}_s}{1+e} \cdot \text{grad } e \qquad (27)$$

If the second term on the right-hand-side of equation (27) is rendered insignificant, the equation is similar to that used by Zaslavsky (1964).

Introducing the soil flux $\vec{q}_s$ as:

$$\vec{q}_s = k_s \frac{\partial u}{\partial e} \cdot \text{grad } e \quad \ldots \quad (28)$$

$$= D_s \cdot \text{grad } e,$$

where

k_s = coefficient of particle conductivity

D_s = particle diffusivity

and writing:

$$\vec{q}_w = \vec{q}_{ws} + \theta \vec{q}_s \quad \ldots \quad (29)$$

where $\vec{q}_{ws}$ = flux of water relative to moving soil particles.

Taking the divergence of both sides, one obtains:

$$\text{div}\,\vec{q}_w = \text{div}\,\vec{q}_{ws} + \text{div}\,\theta\vec{q}_s = -\frac{\partial \theta}{\partial t} \quad \ldots \quad (30)$$

The expanded form of the continuity equation can thus be obtained, with appropriate expansion and substitution as:

$$-\frac{\partial\theta}{\partial t} = \text{div}\,\vec{q}_{ws} + \theta\left[\frac{1}{1+e}\frac{\partial e}{\partial t} + \frac{q_s}{1+e}\cdot\text{grad } e\right] + q_s \cdot \text{grad } e \quad \ldots \quad (31)$$

If the second order terms are ignored, the continuity condition which now accounts for volume change can be stated as:

$$-\frac{\partial\theta}{\partial t} = \text{div}\,\vec{q}_{ws} + \frac{\theta}{1+e}\left[\frac{\partial e}{\partial t} + q_s \cdot \text{grad } e\right] \quad (32)$$

If equation (32) is combined with a modified form of the Darcy relationship to yield the diffusion equation. If q_s is considered small in equation (32), it can be further reduced to:

$$-\frac{\partial\theta}{\partial t} = \text{div}\,\vec{q}_{ws} + \frac{\partial v}{\partial t} \quad \ldots \quad (33)$$

The usefulness and choice of the various analytical expressions derived to study unsaturated flow in expansive soils depends not only on the ability of the investigator to measure or determine the appropriate soil properties, e.g. D k, v etc. but also on the need for precision or accuracy. Some application of the various equations together will be discussed in the next section.

UNSATURATED FLOW PERFORMANCE IN SWELLING SOILS

It is apparent from the previous development that fundamental to the requirements of any of the equations shown, is the need for a proper knowledge of the variation of the diffusion coefficient D with water content θ. In the case of unsaturated flow into low or non-swelling soils where little or no volume change occurs, the characteristic moisture profile development shown in Figure 1 can be expected. However, for cases where volume change upon infiltration becomes significant, or where other mechanisms exist which are not accounted for in the simple formulations provided previously, the moisture profiles as seen in Figure 3 can demonstrate many different shapes.

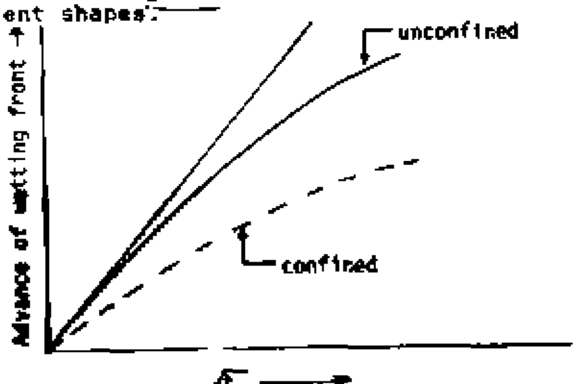

FIG.3: COMPARISON OF MOISTURE PROFILES AND CONFINED AND UNCONFINED FLOW INTO UNSATURATED EXPANSIVE SOILS

In order to establish an appropriate value for D, a matching method can be employed which matches moisture profile with the characteristic diffusivity constant. The influence of various kinds of relationships between θ and D can be seen by writing the right-hand-side of equation (24) in finite difference form (without the second term on the right-hand-side) and solving for certain specific cases governing *θ and D*. *This* simplification is acceptable since $\theta \frac{\partial v}{\partial t}$ does not really enter into or need participate in the characterization of D. The volume change term in equation (24) will affect the numerical value of D but has an insignificant effect on characterizing [shape] the θ-D relationship.

Thus, writing equation (4) as:

$$\frac{\partial\theta}{\partial t} = \frac{1}{(\Delta x)^2}\Big[D_{n-\frac{1}{2}}(\theta_{n+1} + \theta_{n-1} - 2\theta_n) + (D_{n+\frac{1}{2}} - D_{n-\frac{1}{2}})(\theta_{n+1} - \theta_n)\Big] \quad .. \quad (34)$$

where the subscript n here denotes space iteration such that $x_n = n(\Delta x)$. Considering only the adsorption process, five relationships between θ and D have been examined, the results of which are shown in Figure 4. [Wong (1973), Yong and Wong (1973)].

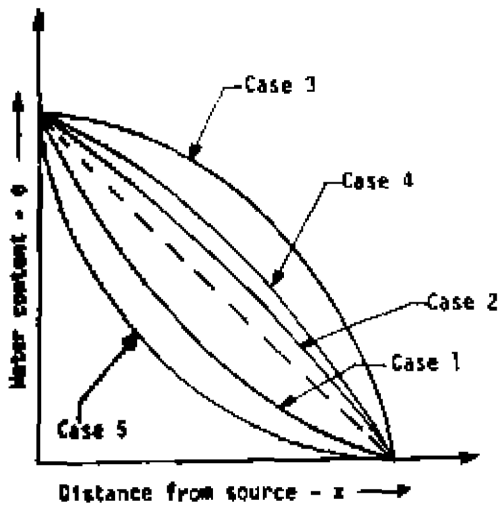

FIG.4: THEORETICAL MOISTURE PROFILES PREDICTED FROM EVALUATION OF DIFFUSE EQUATION

The cases considered in Figure 4 are:

Case 1 D = constant

Case 2 $D = a\theta$, where a = positive constant

Case 3 $D = be^{-c\theta}$ where b and c are positive constants

Case 4 $D = b[1 - e^{-c\theta}]$

Case 5 $D = b_e^{-c\theta}$

In the procedure used to calculate the diffusion coefficient from the moisture profile, the profile is divided into n equal parts in regard to θ between initial θ and saturated θ i.e. θ_i and θ_o, [Wong and Yong (1973)].

Thus, with

$$(\theta_o - \theta_i)/n = \Delta\theta$$

and any value of θ

$$\theta_r = (n-r)\Delta\theta + \theta_i$$

Taking Δθ sufficiently small and a point C as the point $(x(\theta_{r+\frac{1}{2}}), \theta_{r+\frac{1}{2}})$ on the part of the moisture profile curve between A and B. Wong and Yong (1973) show that since θ_c is approximately equal to

$$\theta_{r+\frac{1}{2}},\ D(\theta_c) = D(\theta_{r+\frac{1}{2}});$$

$$D(\theta_c) = D(\theta_{r+\frac{1}{2}})$$

$$= \frac{x(\theta_{r+1}) - x(\theta_r)}{2t\Delta\theta}\left(\int_{\theta_i}^{\theta_{r+\frac{1}{2}}} x\,d\theta\right)$$

$$= \frac{x(\theta_{r+1}) - x(\theta_r)}{2t\Delta\theta}\left(\sum_{j=n-1}^{j=r} x(\theta_j)\Delta\theta + R\right) \quad .. \quad (35)$$

where

$$R = \int_{\theta_i}^{\theta_{n-\frac{1}{2}}} x\,d\theta = x(\theta_i)(\theta_{n-\frac{1}{2}} - \theta_i) \quad .. \quad (36)$$

In low swelling or inactive soils, unsaturated flow occurs in response to the pressure and matric potentials, i.e. ψ_p and ψ_m. The osmotic [or solute] potential ψ_s is insignificant and can be ignored. As the wet front advances in an unsaturated soil, the increase in water content will result in a decrease in soil suction [i.e. an increase in soil water potential]. The time taken for equilibrium to be re-established depends on the initial water content of the unsaturated soil and the potentials ψ_p and ψ_m [Yong and Warkentin (1974)].

In the case of unsaturated flow in expansive soils however, if free swelling is permitted during unsaturated flow, the osmotic component of the total potential, i.e. ψ_π

will decrease to a minimum when the wetting front has progressed beyond the point of interest. Thus, the mechanism causing the unsaturated flow must account for ψ_p, ψ_m and ψ_π. In actual fact, ψ_π will be a continuously varying quantity at any one point of interest. Figure 5 shows the volumetric expansion developed during horizontal unsaturated flow into a swelling soil. The information obtained from Figure 5 can be used in the general diffusion

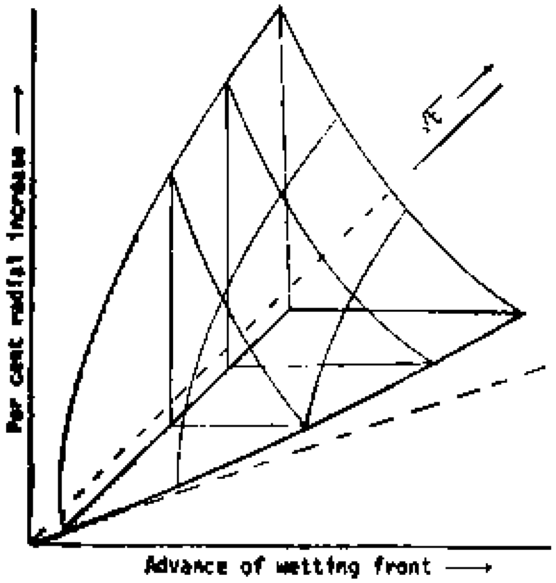

FIG.5: VOLUMETRIC EXPANSION IN SWELLING SOIL DUE TO UNSATURATED FLOW

equation [i.e. equation (24)] to predict the moisture profile for the swelling soil. The comparison between predicted and measured values have been made by Yong and Wong (1973) and may be seen in Figure 6.

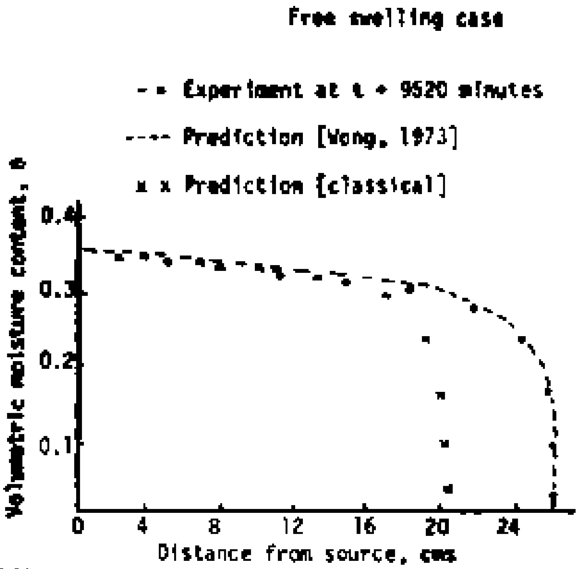

FIG.6: COMPARISON OF ACTUAL AND MEASURED MOISTURE PROFILE

The analysis or prediction of volumetric strains can also be performed by extending equation (19).

If ϕ is the internal pressure responsible for movement of the soil particles in view of the developing fluid flow, we may write:

$$V_{sx} = + k_s \frac{\partial \phi}{\partial x} = + k_s \frac{\partial \phi}{\partial v} \frac{\partial v}{\partial x} \quad .. \quad .. \qquad (37)$$

$$= + D_s \frac{\partial v}{\partial x} \quad .. \quad .. \quad .. \quad .. \qquad (38)$$

where

k_s = soil particle conductivity coefficient analogous to k for fluid flow,

D_s = soil particle diffusivity coefficient.

Since ϕ is responsible for particle movement in unsaturated flow of a swelling soil, the relationship between volumetric strain v and ϕ can be established. Thus:

$D_s = k_s \frac{\partial \phi}{\partial v}$ as used in equation (38).

Equation (38) can now be used in equation (19) to yield:

$$D_s \frac{\partial^2 v}{\partial x^2} = \frac{\partial v}{\partial t} \quad .. \quad .. \quad .. \quad .. \qquad (39)$$

Subject to the boundary condition:

$v = v_o \qquad x = 0 \qquad t > 0$

$v = 0 \qquad x > 0 \qquad t = 0$

the analytical solution will be obtained as:

$$v(x,t) = v_o[1 - \mathrm{erf}(\frac{x}{2\sqrt{D_s t}})] \qquad (40)$$

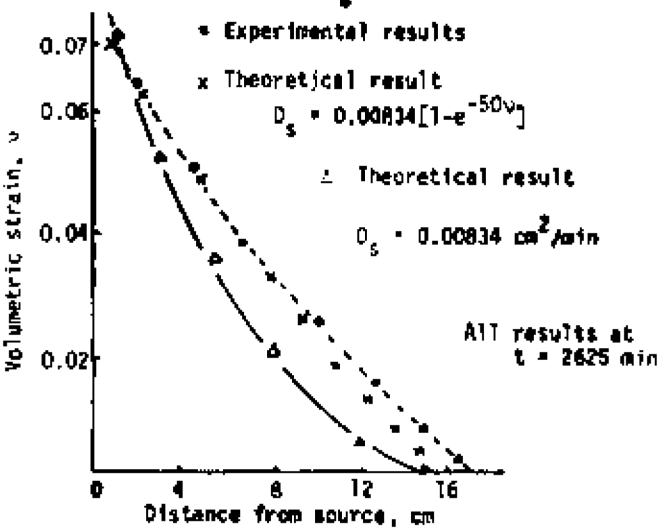

From Yong and Warkentin (1972). Data from Wong (1973)
FIG.7: PREDICTED AND MEASURED VOLUMETRIC STRAINS

The various components of swelling and the variation of swelling force with time have been reported by Wong and Yong (1973). It is of interest to note that the separation between crystalline and osmotic swelling can be made with the technique shown - [see Figure 5 of Wong and Yong (1973)]. The degree of confinement during infiltration [in expansive soils] will provide for varying D(θ) and moisture profiles at any one particular time, in view of the developed swelling forces. This is not unexpected since various characteristic shapes similar to those shown in Figure 5 can be obtained as a function of degree of confinement. Figure 8 shows the schematic for x-$\sqrt{t}$ in view of degree of confinement. These can be directly related to the moisture profiles shown in Figure 9 of Wong and Yong (1973)]. The time rate of penetration of the wet front increases with decreasing restraint. Thus, if D(θ) takes the form represented approximately by Case 3 shown in Figure 4, it is apparent that D(θ) will be larger for the same time period for the same soil, if swelling is allowed to occur during infiltration.

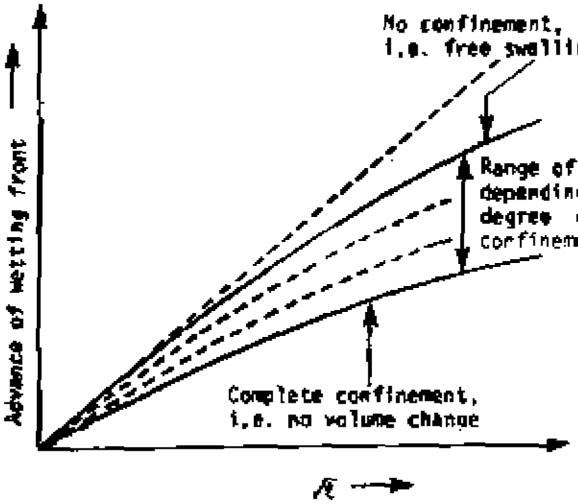

FIG.8: INFLUENCE OF DEGREE OF CONFINEMENT [AND ALLOWED VOLUME CHANGE] ON x-$\sqrt{t}$ CURVES IN UNSATURATED FLOW IN EXPANSIVE SOILS

In the typical case of unconstrained swelling during infiltration, thermocouple psychrometric measurements indicate [as expected from the theory of interpenetration of diffuse ionic layers] that initial soil suction values will decrease with passage of the wet front. The change in soil suction due to penetration or advance of the wet front is shown in Figure 9. As the wet front arrives at a particular location, the initial high soil suction value [due to

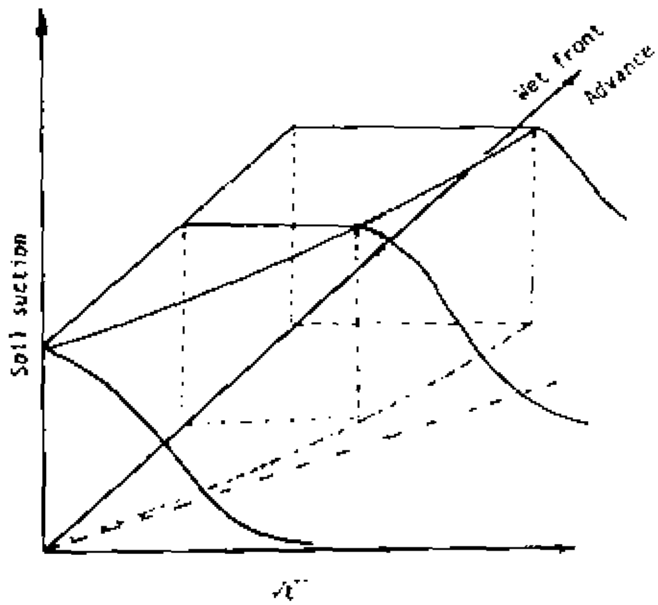

FIG.9: CHANGE IN SOIL SUCTION WITH PENETRATION OF WET FRONT IN EXPANSIVE SOIL

initial unsaturation] begins to decrease. The rate of decrease of the soil suction value is dependent on the degree of constraint applied against swelling, the osmotic potential, and other factors associated with the activity of the soil water system which define the resultant rate of advance of the wet front. For a high swelling clay, and for the condition of unrestrained swelling, the time rate of decrease of the soil suction value is greater than that of a low swelling clay. Thus, the determination of the effective D(θ) becomes difficult as a direct measurement technique. The method suggested for determination of D(θ) using the wet front profile is in all probability the most acceptable and useful overall method for obtaining D(θ). The realization of the wet front profile is one which takes into account the many interactions and interdependencies that occur during unsaturated flow in an expansive soil. Thus such problems as degree of confinement, activity of the system, and other environmental factors pertaining to the infiltration process will demonstrate themselves in the characteristic wet front profile, from which, account for the change in D(θ) can be made. The prediction for unsaturated flow in expansive soils can then proceed using in part, knowledge of the change in soil suction [or soil water potential], the developed wet front profile, the amount of swelling, the change in D(θ) and a proper knowledge of the continuity relationships.

CONCLUSIONS

It is clear that if proper predictions for unsaturated flow in expansive soils is to be made, a proper accounting of the swelling force and the volume changes occurring must be made. Where the physics of the problem have been properly modelled, the analytical solution corresponding to the situation on hand can adequately describe the flow. In part, the continuity relationships in the diffusivity coefficients appear to be the primary components which distinguish expansive soil unsaturated *flow from non-*swelling soil unsaturated flow.

ACKNOWLEDGMENTS

The study was supported under National Research Council of Canada Grant No.A-882. Acknowledgment is made to the author's research students - G. L. Webb, R. K. Chang and H. Y. Wong, who participated fully in the development and conduct of the experiments.

REFERENCES

PHILIP, J. R. and SMILES, D. E., (1969), Kinetics of sorption and volume change in three-component systems. Aust. J. Soil Res., Vol. 7, pp.1-19.

WONG, H. Y., (1973), Unsaturated flow in clay soils. Ph.D. Thesis, Faculty of Eng., McGill University, Montreal.

WONG, H. Y. and YONG, R.N., (1973), A simple solution of some practical engineering problems concerning unsaturated soils. Civ. Eng. Pub. Works Rev. (Great Britain) (in press).

WONG, H. Y. and YONG, R. N., (1973), A study of swelling and swelling force during unsaturated flow in expansive soils. 3rd Int. Conf. on Expansive Soils, Haifa, Israel.

YONG, R. N. and WARKENTIN, B. P., (1972), Unsaturated flow in expansive soils. Proc. Joint Symp. on Fundamentals of Transport Phenomena in Porous Media, University of Guelph, Ontario.

YONG, R. N. and WARKENTIN, B.P., (1974), Soil properties and behaviour. Elsevier Publishing Company, Amsterdam.

YONG, R. N. and WONG, H. Y., (1973), Analytical studies and prediction of unsaturated flow in clay soils. (In preparation).

ZASLAVSKY, D., (1964), Saturated and unsaturated flow equation in an unstable porous medium. Soil Sci., Vol. 98, pp.317-321.

Proc., 3rd Int. Conf. on Expansive Soils, Haifa, Israel. 1973. Vol. I.

A STUDY OF SWELLING AND SWELLING FORCE DURING UNSATURATED FLOW IN EXPANSIVE SOILS

H. Y. Wong, *Research and Development Engineer, Cementation Research Ltd., Rickmansworth, England, and*
R. M. Yong, *Professor and Director, Soil Mechanics Laboratory, McGill University, Canada*

SYNOPSIS Swelling and shrinkage in expansive clay soils as a result of soil water movement always play an important role in foundation design. In the present paper, unsaturated flow tests have been performed in expansive clay soils of cylindrical shape and semi-infinite extent under two limiting conditions. These are: (1) the completely unconfined condition in which the soil is allowed to swell freely along both the radial and the axial direction; and (2) the completely confined condition in which no overall volume change is allowed. In addition to the measurement at various time intervals of the wetting front advance and the moisture profile, the amount of soil swelling along both the radial and the axial direction under the free swelling condition, and the swelling force generated during wetting under the completely confined condition have also been measured. Finally, the possible mechanisms underlying the observed phenomena are suggested.

INTRODUCTION

Swelling and swelling force developed in expansive clay soils as a result of soil water movement always play an important role in foundation design. In the case of saturated soils, it can be studied in conjunction with consolidation, and a lot of work has already been done on that (e.g. Terzaghi, 1943). However, in the case of unsaturated soils, the problem is less well defined since most of the work done has been dealing mainly with small samples of finite extent (e.g. Kassiff and Baker, 1971; Kassiff et al, 1965; Holtz and Gibbs, 1956), and very few with samples of semi-infinite extent. In the latter case, swelling and swelling force will be closely related to the rate of the wetting front advance and the corresponding moisture profile behind it.

In theory, for an expansive soil there are two limiting conditions during wetting. These are: (1) the completely unconfined condition in which the soil is allowed to swell freely along all directions, and (2) the completely confined condition in which no overall volume change is allowed. In practice, the actual condition must be intermediate between these two extremes. However, for fundamental work, it is necessary to study firstly the limiting conditions.

In view of all these considerations, unsaturated flow tests were performed in expansive clay soils of cylindrical shape and of semi-infinite extent under the two above-mentioned limiting conditions. In addition to the measurement at various time intervals of the wetting front advance and the moisture profile, the amount of soil swelling along both the radial and the axial direction under the completely unconfined condition, and the swelling force generated during wetting under the completely confined condition, have also been measured. Finally, the mechanisms underlying the observed phenomena are suggested.

EXPERIMENTATION

Two series of tests were performed, with the first series under a completely unconfined condition while the second one under a perfectly confined one. In each series of tests, water was allowed to flow into a semi-infinite cylindrical soil sample of initially uniform water content through one of its circular ends under zero hydrostatic head.

PHYSICAL PROPERTIES OF TESTING MATERIALS

The clay soil studied was a high swelling one identified as Ste Rosalie clay. In order to vary the activity of the testing samples, the most convenient way was to mix it with different proportions of glass beads. The physical properties of the materials used were summarised in Table 1.

TABLE 1: PHYSICAL PROPERTIES OF MATERIALS USED

Physical Properties / Material Type	Mineral Content	Specific Gravity	Liquid Limit	Plastic Limit	Grain Size Distribution
Ste Rosalie Clay	Mica, Chlorite, with amphibole and a small amount of montmorillonite	2.70	48%	23%	68% < .200 mm 52% < .002 mm
Glass Bead No. 14		2.44			95%-100% with diameter .33 - .42 mm

SAMPLE PREPARATION

50%, 75% and 100% by weight of Ste Rosalie clay passing through a 0.25 mm sieve were mixed respectively with 50%, 25% and 0% by weight of No.14 glass beads into a slurry, with water content just above the corresponding liquid limit. The slurry was de-aired under vacuum and then poured into a split lucite mould of 35mm inside diameter. Constant tapping of the lucite mould was maintained during the pouring process in order to remove trapped air. The slurry was allowed to set in the mould to form a solid sample, which was taken out from the mould after one day's drying and then air-dried. To accelerate aeration, small holes were drilled on the wall of the mould. Leakage of the slurry through these holes was prevented by coating the inside of the wall with nylon mesh.

TEST PROCEDURES

In the two series of tests, de-aired, distilled water was supplied through a constant head device to one end of the sample at zero time, and was maintained at zero hydrostatic head throughout the test. The advance of the wetting front was recorded at different time intervals, and the moisture profile at the end of each test was determined by slicing the sample into sections of 10mm thick, and then finding the water content of each section. All measurements were made at a room temperature of 24 ± 1°C.

TEST SERIES I - The set up of the apparatus was as shown in Fig. 1.

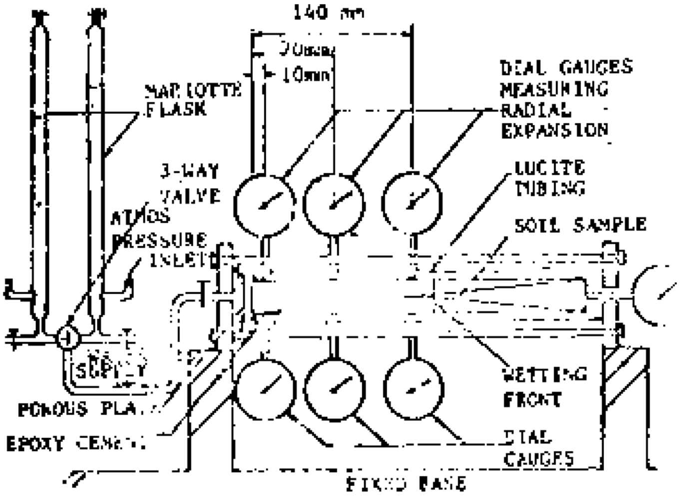

FIG. 1 SET UP OF APPARATUS FOR TEST SERIES I

One end of the sample was first fixed to a porous plate by means of epoxy cement. It was then put into a transparent lucite tubing, and then supported horizontally inside by narrow pieces of sponge which was so soft that its resistance to soil swelling was considered to be negligible. The total amount of axial expansion as well as the radial expansion at points 10, 70 and 140mm respectively from the water sources were measured by means of dial gauges, with the axes of the gauges oriented respectively along the axial and the radial direction. In measuring the radial expansion, the dial gauges, both the top and the bottom ones, at distances 70 and 140mm from the water source could not be put into contact with the soil sample before the start of the test as the axial movement of the sample would tend to destroy the original contact between the gauge and the soil. (This contact was fixed by epoxy cement.) In view of the above fact and also the fact that the subsequent movement of the portion of soil behind the wetting front was relatively small, the dial gauges at these two positions were fixed to the soil when the wetting front was about 10mm away from the position concerned. For a cylindrical soil sample the radial expansion at any point was equal to the increase of diameter at that point and was given by the sum of the readings registered by the top and bottom dial gauges.

Tests were performed on the 50%, 75% and 100% Ste Rosalie clay samples, but moisture profiles at various time durations were only determined for the 50% samples.

The water supply system was the Mariotte Flask type constant head device which consisted of essentially two separate units connected by a three-way valve, which was in turn connected to the water supply line. A device like this enabled a continuous supply of water possible, avoiding the necessity of stopping the supply during the refilling process.

TEST SERIES II - The set up of apparatus for this series of tests was as shown in Fig. 2.

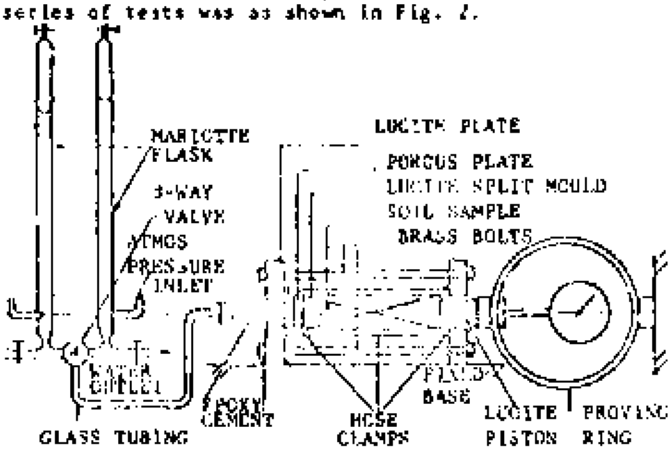

FIG.2 SET UP OF APPARATUS FOR TEST SERIES II

Initially, the sample was confined in a lucite tubing by filling the space between them with melted parowax. However, the samples prepared in this way were still not perfectly confined as expansion along the axial direction and some slight expansion along the radial direction still took place. Better confinement was attained in subsequent tests by confining the sample in a cylindrical lucite split mould. The sample was first cut by the lathe to a size having the same diameter as the internal diameter of the split mould, and was then put into it with good contact between the soil surface and the wall of the split mould maintained by the use of three hose clamps which also served to prevent any lateral swelling of the sample during wetting. The latter method was adopted in the present investigation. With the improved design, further information concerning the swelling force generated along the direction of flow can be obtained by bringing the other end of the cylindrical sample into contact, through a lucite piston, with a proving ring. In this case, the other end of the proving ring and also that of the soil sample holder must be fixed to an immovable base for the measurement of the swelling force (see Fig.2). In order to reduce the frictional force between the wall of the lucite mould and the soil sample, some vaseline was put in between, and any penetration of the vaseline into the sample was prevented by coating the soil sample firstly with a layer of liquid rubber.

As the maximum swelling force measured in the present case was no more than $0.14N/mm^2$ (20 psi), hence the volume change due to the small compression of the proving ring and the elastic expansion of the lucite mould will be quite negligible. It followed that the sample could be taken as completely confined along all directions.

Tests in this series were concentrated on the 50% Ste Rosalie clay samples. This was because the time necessary for one test in the 75% and 100% samples was extremely long. The water supply system was similar to that of test series 1.

DISCUSSION OF TEST RESULTS AND POSSIBLE MECHANISMS

SWELLING IN THE COMPLETELY UNCONFINED CASE

Employing the test results of radial expansion which is a measure of the diameter increase, a 3-dimensional plot is introduced, using distance from water source (x), square root of time ($t^{\frac{1}{2}}$), and radial strain (e_r), which is equal to the radial expansion divided by the original sample diameter, as the three axes. From this plot, a surface will be generated as can be seen from Figs.3a, b and c for samples of 50%, 75% and 100% Ste Rosalie clay respectively. Any point on this surface will give the radial strain at a certain distance from the water source and at a certain time. This will enable a more comprehensive study of the swelling problem possible as at any time t_1, the corresponding variation of the radial strain with distance from water source can be obtained from the curve of intersection of the surface with the plane $t^{\frac{1}{2}}=t_1^{\frac{1}{2}}$. In the same way, the variation of the radial strain with $t^{\frac{1}{2}}$ at a certain distance x_1 from the water source can also be obtained from the curve of intersection of the surface with the plane $x=x_1$.

A study of Figs.3a, b and c shows that in the unconfined case, the rate of swelling at any point is quite fast on first wetting, but drops off very rapidly with time. It can be seen that there exists some sort of exponential relationship between radial strain and square root of time. However, if such an empirical relationship should exist, it must satisfy the following actual conditions;

(1) For $t \leq t_1$, where t_1 is the time required for the wetting front to arrive at a certain point,
$e_r = 0$

(2) For $t \to \infty$ $\quad e_r \to$ a finite quantity

The first condition is obvious since no swelling can occur at a point before wetting. The second one implies that the maximum amount of swelling at any point has an upper limit, which depends upon the soil structure as well as the testing conditions.

It should also be noted that if e_r is to be obtained from a mathematical solution, then for a certain value of x and for $t \leq t_1$, the actual condition of a zero e_r value will be approximated by a mathematical solution which gives insignificantly small e_r values.

With the above two actual conditions in mind, the following empirical equation

$$e_r = \bar{B}\exp(-\bar{b}/(t^{\frac{1}{2}} - t_1^{\frac{1}{2}})) \qquad (1)$$

for time values $t \geq t_1$ seems to be the most appropriate one. $\bar{B}$ and $\bar{b}$ in the above equation are

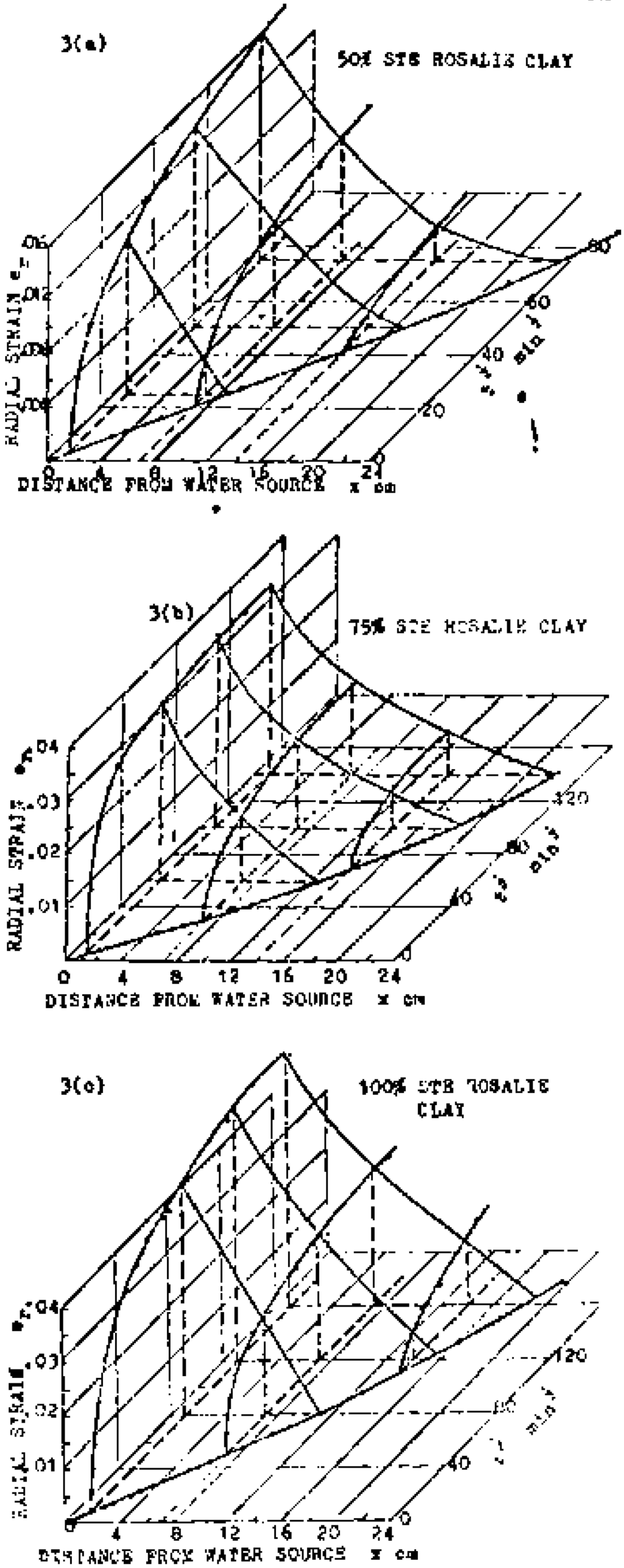

FIG. 3 RADIAL STRAIN SURFACES

parameters which depend on the type of soil, the testing conditions as well as the distance from the water source. In general the parameter $\bar{b}$ will control the magnitude of swelling. It can be seen from the above eq.(1) that as

$$t \to t_1^+ \qquad e_r \to 0$$

$$t \to \infty \qquad e_r \to \bar{B}$$

(the symbol + means that t approaches t_1 from values larger than t_1)

Taking the natural logarithm of both sides of eq.(1)

$$\log e_r = \log \bar{B} - \bar{b}/(t^{\frac{1}{2}} - t_1^{\frac{1}{2}}) \qquad (2)$$

If the above empirical relationship is to hold, a plotting of $\log e_r$ (or $\log_{10} e_r$) versus $1/(t^{\frac{1}{2}} - t_1^{\frac{1}{2}})$ should give a straight line. By plotting the test results of the various types of samples in this way at various values of t_1 (i.e. at various positions of the soil sample) as in Figs.4a, b and c, it can be seen that two intersecting straight lines are obtained instead of only one. This striking result suggests that there might be two distinct stages of swelling, each following the same form of functional relationship, but with different $\bar{B}$ and $\bar{b}$ parameters, as the mechanisms involved in each phase of swelling will be different.

According to Norrish (1954), swelling takes place in two distinct ways, with crystalline swelling in the first stage, and osmotic swelling in the second one. Chang and Warkentin (1966) classified these as structural swell and normal swell, with some of the pores not filled in the stage of structural swell, and the sample fully saturated in the stage of normal swell. For compacted clay, swelling tendency, according to Seed, Mitchell and Chan (1961), may be classified into two general categories: physico-chemical and mechanical. The mechanism of mechanical swelling concerning the bending of clay plates has also been proposed by Terzaghi (1931). In the present case, as the soil sample is prepared by drying, large capillary force will be induced, causing the bending of clay plates. These will straighten again on the release of the capillary pressure during the process of wetting.

In view of the above considerations, mechanical and crystalline swelling seem to be the dominating one in the first stage while osmotic (or normal) swelling in the second one. It is obvious that the dividing line between these two stages cannot be too distinct; some osmotic swelling might have already started in the later part of the first stage.

Further experimental support for the above two-stage swelling mechanism can be obtained by plotting volumetric strain (i.e. swelling per unit gross soil volume) against volumetric water content as in Fig.5 for the various samples. The graph shows that the increase of volumetric strain will be approximately equal to the corresponding increase of volumetric water content only when the amount of swelling has exceeded about 40% of the total. Since the amount of volume change will be equal to the amount of water absorbed in the case of osmotic swelling, hence the above result indicates that osmotic swelling will be dominating in the later stage of the swelling process at a certain position in the soil sample during the advance of the wetting front.

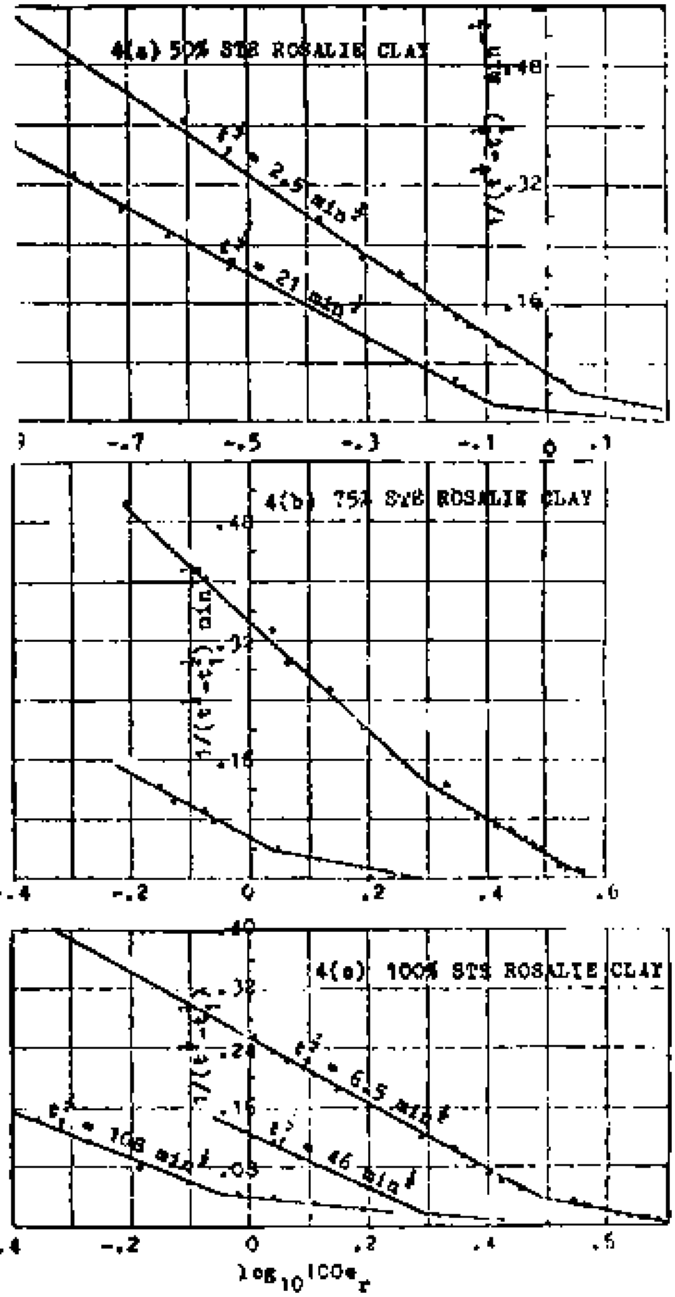

FIG.4 VARIATION OF $LOG_{10} e_r$ WITH $t^{\frac{1}{2}}$

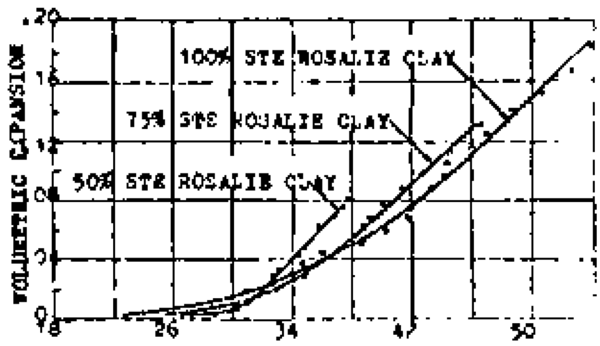

FIG.5 VARIATION OF SWELLING WITH WATER CONTENT

Considering in a more quantitative manner, the $\bar{B}$ value, which represents the total amount of radial strain at a certain point from the water source should be evaluated graphically from Figs.4a, b and c. Because of the two stage swelling, there will be two $\bar{B}$ values (i.e. $\bar{B}_{stage\ 1}$ and $\bar{B}_{stage\ 2}$). The total amount of radial strain (i.e. $\bar{B}_{stage\ 1} + \bar{B}_{stage\ 2}$) is given by the intercept on the $\log_{10}e_r$ axis of the second straight line branch of the $\log_{10}e_r$ versus $1/(t^{\frac{1}{2}} - t_i^{\frac{1}{2}})$ curve in Figs.4a, b and c.

In theory, the total amount of swelling for a given type of soil should be the same everywhere when t approaches infinity. As the time value involved in the present tests is not sufficiently large, it can be expected that the $\bar{B}$ value for a point further away from the water source will have a smaller value than that of a nearer point, as can be seen from Figs.4a, b and c. However, the curves for various points do show some general tendency to converge into a single point on the $\log_{10}e_r$ axis. Of course, a more precise value can only be obtained by running the test for an infinitely long time.

Furthermore, by producing the first straight line branch beyond the turning point, its intercept on the $\log_{10}e_r$ axis should give a very rough estimate of the amount of the first stage swelling (i.e. $\bar{B}_{stage\ 1}$). Subtracting this from the total swelling (i.e. the intercept of the second straight line branch on the $\log_{10}e_r$ axis, $\bar{B}_{stage\ 1} + \bar{B}_{stage\ 2}$) the amount of radial strain during the second stage (i.e. $\bar{B}_{stage\ 2}$) can also be very roughly estimated. Owing to the various amounts of overlapping of those two stages at various points, the exact B value for each stage will be extremely difficult to determine.

Comparing the rate of swelling at various positions after the elapse of the same value of $(t^{\frac{1}{2}} - t_i^{\frac{1}{2}})$, it can be seen that for points further away from the water source, the rate of swelling becomes progressively slower. This can be expected because of the decrease of the rate of wetting front advance, and hence the rate of water supplied. The rate of swelling can also be compared in a more quantitative manner by measuring the corresponding $\bar{b}$ values from Figs.4a, b and c. $\bar{b}$ is just the slope of the straight line portion of the $\log_{10}e_r$ versus $1/(t^{\frac{1}{2}}-t_i^{\frac{1}{2}})$ curve divided by $\log_{10}e$. It varies with the type of soil as well as the stage of swelling. However, owing to the very empirical nature of eq.(1), no exact physical significance can be attached to this parameter.

For the axial expansion data, as only the measurement of the total axial expansion over the whole wetted portion has been made (see Fig. 6), therefore only the average value ($\bar{e}_a$) over this portion is known. Accordingly, this should be compared with the corresponding average radial strain ($\bar{e}_r$) over the same wetted portion. The $\bar{e}_a$ values at various stages of wetting can be easily obtained from Fig.6 by dividing the total axial expansion by the corresponding length of the wetted portion (i.e. the distance of the wetting front from the water source). As for the corresponding $\bar{e}_r$ values, this is equal to the area under the e_r versus x curve at a certain time t (when the wetting front is at X) divided by X. The $\bar{e}_r$ versus x curve is obtained from Figs.3a, b and c by intersecting the radial strain surface with the $t^{\frac{1}{2}}$ = constant plane.

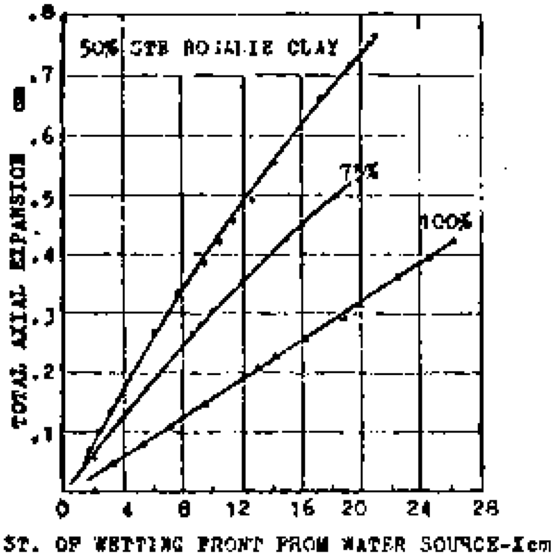

FIG. 6 TOTAL AXIAL EXPANSION

The $\bar{e}_a$ and $\bar{e}_r$ values at various stages of wetting are summarised in Table II.

TABLE II

$\bar{e}_a$ AND $\bar{e}_r$ VALUES FOR VARIOUS STE ROSALIE CLAY SAMPLES

Type of Sample	Wetting Front Advance, X, cm	$\bar{e}_a$	$\bar{e}_r$	$\bar{e}_a/\bar{e}_r$
50% Ste	8.6	.0158	.00581	2.7[illegible]0
Rosalie	17.0	.0159	.00593	[illegible]
Clay	23.0	.0158	.00579	2.7[illegible]
75% Ste	12.6	.0289	.01540	1.5[illegible]
Rosalie	18.6	.0269	.01490	1.50[illegible]
Clay	22.1	.0252	.01390	1.6[illegible]
100% Ste	11.0	.0391	.02430	1.6[illegible]
Rosalie	15.1	.0384	.02370	1.[illegible]
Clay	18.6	.0371	.02260	1.[illegible]

It should be noted that for a given sample at various stages of wetting, the ratio $\bar{e}_a/\bar{e}_r$ is practically constant, but $\bar{e}_a$ is considerably larger than $\bar{e}_r$. [illegible] latter phenomenon means that the percentage of [illegible] is larger along the direction of water flow. [illegible] quite expectable according to the previous proposed mechanisms since the initially bent clay particles will have a higher tendency to straighten along the direction of water flow on wetting.

SWELLING FORCE IN THE COMPLETELY CONFINED CASE

In the completely confined sample, [illegible] increase of soil volume cannot [illegible] swelling force developed during the flow process [illegible] play a dominant role. Fig.7 shows the variation [illegible] the time of the total swelling force developed along the direction of water flow. This indicates [illegible] rapid, but then a more gradual in[illegible]. The first rapid increase is probably [illegible] swelling force developed from the hydration [illegible] clay plates and the exchangeable cations (i.e. [illegible] crystalline swelling proposed by Norrish, 1954), tending to push the clay particles apart, and also from the tendency of the clay plates to straighten (i.e. the mechanical swelling proposed by Terzaghi, 1931; and Seed et al, 1961). The subsequent gradual

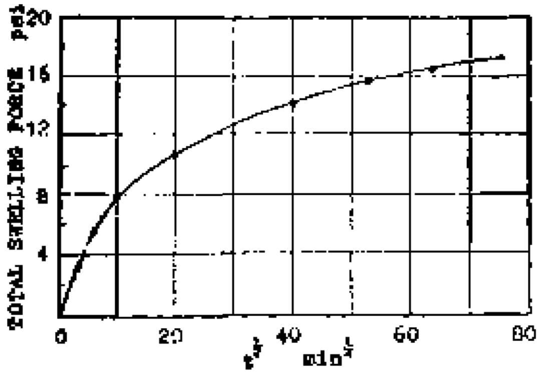

FIG.7 VARIATION OF SWELLING FORCE WITH TIME

increase is probably due to the filling of the capillary pores, resulting in a tendency of osmotic swelling. The above mechanisms seem to be the valid ones since crystalline and mechanical swelling are much faster than the filling of the capillary pores. At the same time, the possible rearrangement of the soil particles along the direction of water flow (e.g. Miller and Low, 1963) will result in a decrease of swelling force in this direction, and this can further decrease the rate of increase of the total swelling force at large time values in the present case.

It is also worthwhile to mention that in the testing of a shorter sample, the swelling force does show a gradual decrease a few days after the whole length of soil sample has been wetted. This is very similar to the aging effect as observed by Kassiff and Baker (1971). However, the amount of data available is not enough to draw any specific conclusion.

WETTING FRONT ADVANCE AND SOIL MOISTURE DISTRIBUTION

The importance of a knowledge of the amount of swelling and the swelling force as a result of wetting in foundation design is obvious. From the previous data, it can be seen that both the total amount of swelling and the swelling force are dependent upon the length of the wetted portion (i.e. the position of the wetting front), which, in turn, is affected by the degree of confinement.

In addition, the mechanical properties of a given type of soil also depend on the water content. As only the water content in that portion of soil behind the wetting front is altered, it is therefore also necessary to study the corresponding water content distribution at various stages of wetting.

Fig.8 shows a comparison of the variation of the wetting front advance with the square root of time under the two limiting testing conditions. From the figure, it can be seen that

(1) the wetting front advance versus square root of time curves (i.e. X versus $t^{\frac{1}{2}}$ curves) for both cases start to bend continuously downward after a certain time interval, with the completely confined case starting much earlier,

(2) The rate of wetting front advance is much slower in the completely confined case.

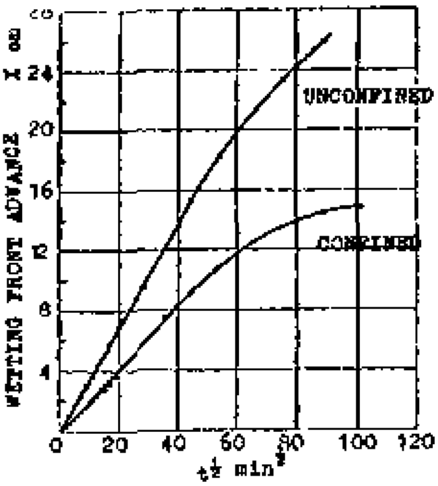

FIG.8 WETTING FRONT ADVANCE

The above phenomena can be explained as follows. As the linear relationship between wetting front advance and square root of time is commonly used as a test of the uniformity of packing of a non-swelling medium in an unsaturated flow system (e.g. Nielsen et al, 1962; Jackson et al, 1962), a deviation from this linear relationship implies therefore a non-uniform packing in a non-swelling medium. In the case of a swelling medium, this deviation might imply a swelling which gives rise to an extension of the diffuse double layer as well as a pore geometry change, as proposed by Rawlins and Gardner (1963), and Christenson and Ferguson (1966). In general, if swelling results in a larger effective mean pore size, the X versus $t^{\frac{1}{2}}$ curve will bend continuously upward; and if a smaller effective mean pore size results, then the reverse will happen. The change in curvature of this curve will be continuously along either direction since swelling of a soil colloid is a time-dependent phenomenon, as recognised by many workers (e.g. Norrish, 1954; Rowell, 1963), and as indicated in the present test results (e.g. Figs.3a, b and c, Fig.6 and Fig.7).

With the extension of the diffuse double layer, more water molecules will be under the influence of the clay plates and the exchangeable cations. This water is called the adsorbed water which has, according to Kemper (1960), a viscosity value higher than the normal water, or according to Low (1961), Miller and Low (1963), a quasi-crystalline structure. The postulate by Yong and Warkentin (1966) that the driving forces of flow must exceed these forces holding water to the soil particles, and that the mid-plane potential between these two particles must be exceeded before liquid transfer can occur is in line with that proposed by Low (1961), and that shown experimentally by Miller and Low (1963). Alternatively, Michael and Lin (1954), and Kemper (1960) have shown experimentally that electro-osmotic counter flow would be operating, and this would naturally increase with the extension of the diffuse double layer. As for pore geometry change, a mechanism of void plugging resulting from particle movement has been proposed by Hansbo (1960) and Martin (1962).

From the above considerations, it can be seen that a continuous reduction in the effective mean pore size will result if the overall volume is to remain the same as in the completely confined case because the continuous increase of swelling force will result in an increase of mid-plane potential, and finally an equivalent smaller effective mean pore size. For the free swelling case, this reduction will be counterbalanced somewhat by the increase of the overall volume. This explains quite satisfactorily the phenomena: (1) the starting of the curvilinear relationship between X and $t^{\frac{1}{2}}$ at a much later stage in the completely unconfined 50% Ste Rosalie clay sample, and at an earlier stage in the completely confined one, and (2) the faster rate of wetting front advance in the completely unconfined case.

The time dependent nature of the swelling phenomena will also be reflected in the shape of the moisture profiles at various time durations as shown in Fig.9.

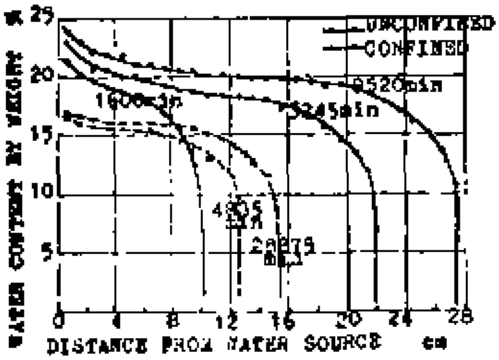

FIG. 9 SOIL MOISTURE PROFILE

Because of the continuous swelling of the sample, water content at any point, on a volumetric basis, might decrease with time even though the mass of water per unit mass of soil is increasing; in the same manner, the water content at a point near the water source might be lower than that at the point further away. In order to avoid the above awkward situation, water content on a mass basis has been used here for comparison.

As can be expected, Fig.9 indicates that:

(1) for approximately the same time of wetting and at the same distance from the wetting source, the water content in the unconfined case is considerably higher than that in the completely confined case; and

(2) the water content at any point increases continuously with time, and the rate of increase is much faster in the unconfined case.

However, for practical considerations, the water content distribution data must be able to be related to the corresponding suction distribution. In view of the difficulties of measuring the suction profile directly during the wetting of a semi-infinite sample, suction tests have been performed separately on small thin samples, with the corresponding volume change also measured in the unconfined case. Fig.10 is a 3-dimensional plot, showing the relationship between volumetric expansion, water content and suction, for the unconfined case during the wetting cycle. It should be noted that in the present case, there is no longer a unique relationship between water content and suction for a given sample even for the wetting cycle alone. The volumetric expansion parameter must also be taken into account. In order that the suction-water content relationship as determined from suction tests on small finite samples to be

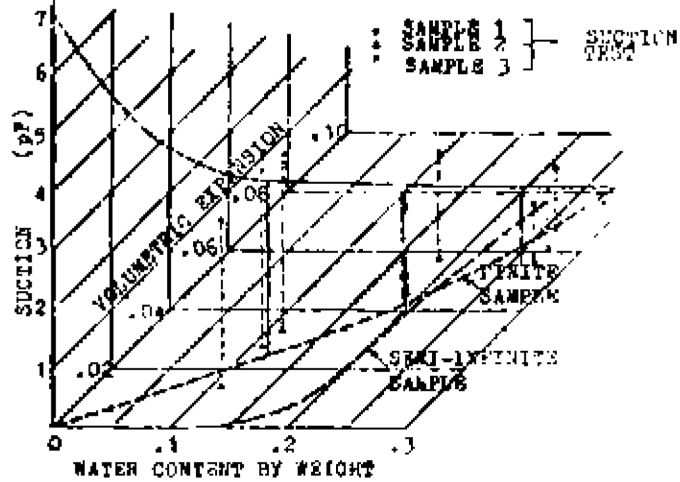

FIG.10 VARIATION OF SUCTION WITH WATER CONTENT AND SOIL SWELLING

applicable to the semi-infinite sample during the unsaturated flow test, the volumetric expansion-water content relationship must be identical in both types of tests. From Fig.3a and Table II, the volumetric expansion profile can be obtained for a given water content profile. From these, the volumetric expansion-water content relationship for the wetting of a semi-infinite sample can be deduced and compared with the corresponding one for the suction test, as shown in Fig.10. The two curves differ considerably, indicating that the suction test results are not directly applicable. The above difference is probably due to the difference in nature of the flow process in these two types of tests. In the wetting of a semi-infinite sample, the flow is always at a transient state because the sample is of semi-infinite extent as far as the flow process is concerned. On the other hand, the water content in a suction test can be determined at a state of equilibrium at which no further flow of water will occur because of the finite thickness of the sample. Also bearing in mind that swelling is a time-dependent process, the above deviation is quite in line with the mechanisms proposed so far. This difference in nature of the flow process in these two types of tests certainly will have similar effects on the completely confined case, but only to a different extent.

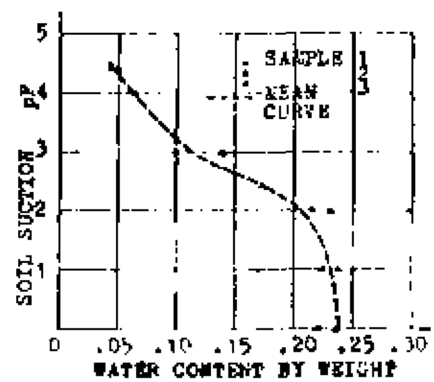

FIG.11
SUCTION TEST RESULTS (COMPLETELY CONFINED CASE)

Fig. 11 shows the relationship between suction and water content for the completely confined case.

In these tests, small samples of finite thickness were confined by parowax on all sides except the contact plane with the porous plate. Expansion along the vertical direction was further prevented by adding dead weights on the top. This method of confinement was fairly successful for samples at high suction values. Some volumetric expansion was visible in spite of the fact that the amount of dead weight was increased continuously. The suction data thus obtained can again only offer a rather qualitative indication of the actual value in the semi-infinite sample during wetting.

CONCLUSIONS

It is obvious from the present test results on the wetting of semi-infinite expansive soil samples that:

(1) the rate of wetting is affected considerably by the degree of confinement,
(2) both the total amount of swelling and the magnitude of the swelling force developed increase with the increase of the length of the wetted portion, which, in turn, increases with time,
(3) the rate of swelling for a given sample at any point is dependent upon the time of wetting as well as the moisture condition of the neighbouring points, and
(4) the swelling profile at any instant assumes a concave shape (i.e. the percent swell decreases rapidly with the increase of distance from the wetting source).

Furthermore, the suction values in a semi-infinite expansive sample during wetting cannot be deduced indirectly from the conventional laboratory test on small samples of finite thickness as the flow process in the former case is always at a transient state, while the latter will approach an equilibrium state during the final stage.

These results are of practical significance for foundation design in expansive clay soils as the active layer of the foundation soil usually can be considered as of semi-infinite extent as far as the wetting process is concerned. At the same time, normal practice for foundation design on such soils is to determine the percentage of vertical swell under a certain vertical confining stress on a sample of finite thickness taken from various depths inside the active zone. Usually, the sample is soaked for a maximum period of only a few days; the vertical confining stress is equal to the corresponding overburden pressure; and the sample thickness in most cases varies from 12-50 mm (e.g. Holtz and Gibbs, 1956; Parry, 1966; Alpan, 1957; Kassiff, Livneh and Wiseman, 1969). The total expected swell is then obtained by integrating the percent swell obtained from the swelling tests with depth. As for the relationship between suction and water content, this is usually determined separately on samples of finite thickness by such methods as suction plate, pressure membrane, etc. (see Croney et al, 1952).

All these together with the present test results indicate that foundation design on expansive clay soils may be further improved along the following lines:

(1) to perform swelling test on a longer sample with the initial water content distribution equal to that in the site,
(2) to vary the lateral confinement according to the appropriate condition in the site.
(3) to measure directly, during the wetting of a semi-infinite sample, the corresponding suction profile at various time intervals.

REFERENCES

ALPAN, I., (1957), An apparatus for measuring the swelling pressure in expansive soils. Proc, 4th I.C.S.M.F.E., Vol.1, London, 3-5.

CHANG, R.K. and WARKENTIN, B.P., (1966), Volume change of compacted clay soil aggregates. Soil Sci., Vol.105, 106-111.

CHRISTENSON, D.R. and FERGUSON, H., (1966), The effect of interactions of salts and clays on unsaturated water flow. Soil Sci.Soc. Amer. Proc., Vol.30, 549-553.

CRONEY, D., COLEMAN, J.D. and BRIDGE, P.M., (1952), The suction of moisture held in soil and other porous materials. Road Research Technical Paper No. 24, Road Research Laboratory, London.

HANSBO, S., (1960), Consolidation of clay, with special reference to influence of vertical sand drains. Swed. Geotech. Inst. Proc., Vol.18, 160pp.

HOLTZ, W.G. and GIBBS, H.J., (1956), Engineering properties of expansive clays. Paper No. 2814, Trans. ASCE, Vol.121, pp.647.

JACKSON, R.D., REGINATO, R.J. and REEVES, W.E., (1962), A mechanized device for packing soil columns. USDA-ARS, 41-52.

KASSIFF, G. and BAKER, R., (1971), Aging effect on swelling potential of compacted clays. J. Soil Mech. Found. Div., ASCE, Vol.97, SM3, 529-540.

KASSIFF, G., KOMORNIK, A., WISEMEN, G. and ZEITEN, J.G., (1965), Studies and design criteria for structures on expansive clay. Symposium on Engineering Effects of Moisture Changes in Soils, Texas A and M Press, Texas.

KASSIFF, G., LIVNEH, M. and WISEMAN, G., (1969), Pavements on Expansive Clays. Jerusalem Academic Press.

JONES, H.E. and KOHNKE, H., (1952), The influence of soil moisture tension on vapour movement of soil water. Soil Sci. Soc. Amer., Vol. 16, 245-248.

KEMPER, W.D., (1960), Water and ion movement in thin films as influenced by the electrostatic charge and diffuse layer of cations associated with clay mineral surfaces. Soil Sci. Soc. Amer. Proc., Vol.24, 10-16.

LOW, P.F., (1961), Physical chemistry of clay-water interaction. Advance in Agronomy, Vol.13, 269-327.

MARTIN, R.T., (1962), Adsorbed water on clays A review. Clays and Clay Minerals, Vol.11, 28-70.

MICHAEL, A.S. and LIN, C.S., (1954), The permeability of kaolinite. Industrial and Engineering Chemistry, Vol.46, No.6, 1239-1246.

MILLER, R.J. and LOW, P.F., (1963), Threshold gradient for water flow in clay systems. Soil Sci. Soc. Amer. Proc., Vol.27, 605-609.

NIELSEN, D.R., BIGGAR, A.W. and DAVIDSON, J.M., (1962), Experimental consideration of diffusion analysis in unsaturated flow problems. Soil Sci. Soc. Amer. Proc., Vol.26, 107-111.

NORRISH, K., (1954), The swelling of montmorillonite. Disc. Faraday Soc., Vol.18, 120-134.

PARRY, R.H.G. (1966), Classification test for shrinkage and swelling soils. Civil Engineering and Public Works Review, Vol.61, June, London, 719-721.

RAWLINS, S.L. and GARDNER, W.H., (1963), A test of the validity of the diffusion equation for unsaturated flow of soil water. Soil Sci. Soc. Amer. Proc., Vol.27, 507-511.

ROWELL, D.L., (1963), Effect of electrolyte concentration on the swellings of orientated aggregates of montmorillonite. Soil Sci., Vol.96, 368-374.

SEED, H.B., MITCHELL, J.K. and CHAN, C.K., (1961), Studies of swell and swell pressure characteristics of compacted clays. Highway Res. Bull. 313, 12-39.

TERZAGHI, K., (1931), The influence of elasticity and permeability on the swelling of two-phase system. Colloid Chemistry, Vol.3, 65-88.

TERZAGHI, K., (1943), Theoretical Soil Mechanics. New York, John Wiley and Sons.

YONG, R.N. and WARKENTIN, B.P., (1966), Introduction to Soil Behaviours. The Macmillan Company, New York.

ACKNOWLEDGEMENT

The research was conducted under a National Research Council grant, Canada (R.N. Yong, Grantee) at McGill University.

Engineering problems in unsaturated soils

H Y Wong MSc(Eng) PhD CEng MICE
Research and Development Engineer, Cementation Research Ltd

R N Yong MEng PhD MICE MASCE
Professor and Director, Soil Mechanics Laboratory, McGill University, Montreal

In highway and foundation designs, unsaturated soils are usually encountered near the surface as a result of seasonal wetting and drying. Under such conditions, the parameters governing soil water movement will be of utmost importance as these will determine the soil water content, which will in turn affect the soil strength. For such practical problems as the infiltration of water into unprotected natural slopes during a heavy rainstorm or the prepounding of foundation on soils of a high potential to swell or to collapse, it is essential that a knowledge of water content distribution at any instant be known, in as much as the stability of the unprotected slope or the subsequent bearing capacity of the prepounded foundation may be conditioned accordingly.

In general, the soil water movement and hence water content distribution for a given type of soil will be completely specified by its suction (ψ) and permeability (k) values, which are functions of water content (θ) only in the case of a stable porous medium (eg a granular soil or a fairly low swelling clay soil). Under such conditions, a combination of Darcy's law and the continuity equation will result in the classical concentration dependent-type diffusion equation. Ideally, if both suction and permeability have known functional relationships with water content for a given type of soil, it would be advisable to introduce a new parameter, D, which is a function of suction, permeability and water content, and hence a function of water content only.

The introduction of the parameter, D, identified as the soil water diffusivity, is a matter of mathematical convenience with little tenuous physical significance. The mathematical relationship includes few parameters with the complete solution being controlled by only one single parameter. Much work has been done, aiming at deducing this soil water diffusivity parameter using various types of test. However, only limited success has been achieved. The testing methods are either too involved or calculation procedures are too cumbersome and tedious.

This paper presents a review of the common methods of determining this soil water diffusivity parameter, together with a discussion of their respective shortcomings. A modified method involving a very simple testing technique as well as simple calculation procedures is proposed. The suitability of this method is then assessed by testing its reproducibility, using different sets of test data from the same type of soil. The means for applying these to the solution of practical engineering problems such as those mentioned earlier are subsequently considered.

General equations governing flow in unsaturated soils

In the case of a stable porous medium, Darcy's law can be applied to give the flow velocity in the one dimensional case as

$$v = -k\frac{\partial \psi}{\partial x} \qquad \ldots\ldots\ldots [1]$$

where x = horizontal co-ordinate axis.
This, when combining with the continuity equation

$$\frac{\partial \theta}{\partial t} = -\frac{\partial v}{\partial x} \qquad \ldots\ldots\ldots [2]$$

will give the classical concentration dependent-type diffusion equation

$$\frac{\partial \theta}{\partial t} = \frac{\partial}{\partial x}\left(D(\theta)\frac{\partial \theta}{\partial x}\right) \qquad \ldots\ldots\ldots [3a]$$

with $D(\theta) = k(\theta)\frac{d\psi}{d\theta}$ .... [4]

and t = time

In three-dimensional form:

$$\frac{\partial \theta}{\partial t} = \nabla\cdot(D(\theta)\nabla\theta) \qquad \ldots\ldots\ldots [3b]$$

A review of the methods of soil water diffusivity determination

In theory, the value of diffusivity (D) at any water content value (θ) can be calculated from equation [4] provided that the corresponding values of soil suction (ψ) and soil water permeability (k) are known. This requires the measurement of both the soil suction and the soil water permeability at various water contents on identical samples.

A direct method (1) which calculates the soil water diffusivity from the pressure plate outflow data involves the application of a small differential pressure across a soil sample with the measurement of the volume of water flowing out from the sample at various time intervals. By plotting the experimental outflow data in the form of $\log(Q_{\infty} - Q_t)$ versus t, where Q_{∞} is the total amount of water outflow and Q_t is that at time t, a straight line should be obtained according to the approximate solution of the diffusion equation [3a]. The mean soil water diffusivity value within a certain range of moisture content can then be calculated from the slope of this best-fitted straight line.

The above method has been improved by Miller and Elrick (2) who attempted to include the effect of plate (or membrane) impedance, and by Kunze and Kirkham (3) who used only the initial portion of the outflow data in order to minimize the effect of the change in D with θ.

In general, there are two shortcomings of the above method. Firstly, the experimental procedures require skilled techniques for the successful operation. Secondly, the basic assumption of a constant D in the solution of the partial differential equation [3a] is a fundamental weakness. The initial portion of the outflow curve is sensitive to plate impedance effect [4] which might render this initial portion of the curve non-linear.

Another approach [5] expresses the soil water diffusivity (D) as a function of some of the parameters which could be evaluated from an experimentally determined soil moisture profile (ie moisture content—distance curve). This can be done by introducing the Boltzmann transformation

$$\eta_i = x/t^{\frac{1}{2}} = \eta_i(\theta) \qquad \ldots\ldots [5]$$

into the classical diffusion equation [3a] to give

$$-\frac{\eta_i}{2}\frac{d\theta}{d\eta_i} = \frac{d}{d\eta_i}\left(D(\theta)\frac{d\theta}{d\eta_i}\right) \qquad \ldots\ldots [6]$$

and integrating with respect to η_i to give

$$D(\theta_1) = -\frac{1}{2}\left(\frac{d\eta_i}{d\theta}\right)_{\theta_1}\int_{\theta_i}^{\theta_1}\eta_i\,d\theta \qquad \ldots\ldots [7]$$

where θ_i is the initial water content of the soil sample. At a certain time, t,

$$D(\theta_1) = -\frac{1}{2t}\left(\frac{dx}{d\theta}\right)_{\theta_1}\int_{\theta_i}^{\theta_1} x\,d\theta \qquad \ldots\ldots [8]$$

where $\left(\frac{dx}{d\theta}\right)_{\theta_1}$ is the slope of the θ versus x curve at the point $(x(\theta_1), \theta_1)$, and $\int_{\theta_i}^{\theta_1} x\,d\theta$ is the area under the θ versus x curve, bounded by the lines $\theta = \theta_1$, $\theta = \theta_i$ and the θ-axis.

The advantage of this method over the previous one is its simplicity in the experimental procedures. Furthermore, the only additional assumption involved in the solution of the classical diffusion equation is the Boltzmann transformation

$$\eta = x/t^{\frac{1}{2}} = \eta(\theta)$$

which physically implies that the wetting front advance must vary linearly with the square root of time, and this is always true in a stable porous medium with horizontal water flow. However, for water contents at either end of the range, this method of calculation becomes less stable.

Finally, a very practical but only approximate method has been proposed by Aitchison, Russam and Richards [6]. By measuring the in situ suction at a reference point at times t and $(t + \Delta t)$, and also the mean suction over this time period Δt at six equal spaced points which are at equal distance from the reference point along the three major coordinate axes, the means of water diffusivity (D) corresponding to the mean suction (or mean water content) at this point can be evaluated from an approximate solution of the three-dimensional diffusion equation [3b]. This can also be applied to laboratory work as well as one- or two-dimensional cases.

Present method of calculation

The present proposed method of calculation is basically a simplified version of that proposed by Bruce and Klute [5], but with all the calculations arranged systematically in tabular form. This can now be done most conveniently by a desk calculator or by a high-speed electronic computer. The principles of the present method are given below.

Consider any experimentally determined water content-distance curve, as shown in Fig 1, with the maximum and minimum water content value respectively equal to θ_o and θ_i. (The maximum water content value θ_o here is usually equal to the saturated water content value). For convenience of calculation and presentation, replace the variable θ by $\bar\theta$ such that

$$\bar\theta = \theta/\theta_o$$

which is just equal to the degree of saturation if θ_o is the saturated water content. Divide $(\bar\theta_o - \bar\theta_i)$ into n equal parts (or $\bar\theta_o$ into n equal parts if θ_i is small) such that

$$(\bar\theta_o - \bar\theta_i)/n = \Delta\bar\theta \qquad \ldots\ldots [9]$$

and

$$\bar\theta_r = (n-r)\Delta\bar\theta + \bar\theta_i \qquad \ldots\ldots [10]$$

The lines $\bar\theta = \bar\theta_r$ and $\bar\theta = \bar\theta_{r+1}$ will now cut the water content-distance curve at A and B respectively (see Fig 1). The corresponding abscissa of A and B will be $x(\bar\theta_r)$ and $x(\bar\theta_{r+1})$. Since the part of the curve between A and B is continuous and differentiable, therefore, by the mean value theorem, there will be a point C in between A and B such that the tangent (ie slope) at C is equal to the slope of the straight line joining A and B, ie

$$\left(\frac{d\bar\theta}{dx}\right)_{\bar\theta_c} = \frac{-\Delta\bar\theta}{x(\bar\theta_{r+1}) - x(\bar\theta_r)} \qquad [11]$$

By taking $\Delta\bar\theta$ sufficiently small, C can be taken approximately as the point $(x(\bar\theta_{r+\frac{1}{2}}), \bar\theta_{r+\frac{1}{2}})$ on the part of the curve between A and B. Substituting equation [11] into equation [8]

$$D(\bar\theta_c) = D(\bar\theta_{r+\frac{1}{2}}) = \frac{x(\bar\theta_{r+1}) - x(\bar\theta_r)}{2t\Delta\bar\theta}\int_{\bar\theta_i}^{\bar\theta_r} x\,d\bar\theta$$

$$= \frac{x(\bar\theta_{r+1}) - x(\bar\theta_r)}{2t\Delta\bar\theta}\left(\sum_{s=r+1}^{n} x(\bar\theta_s)\Delta\bar\theta + R\right) \qquad [12]$$

where

$$R = \int_{\bar\theta_i}^{\bar\theta_n} x\,d\bar\theta \approx x(\bar\theta_n)(\bar\theta_n - \bar\theta_i) \qquad [13]$$

As the extreme positions of C are A and B, therefore the

Fig 1. Hypothetical water content-distance curve

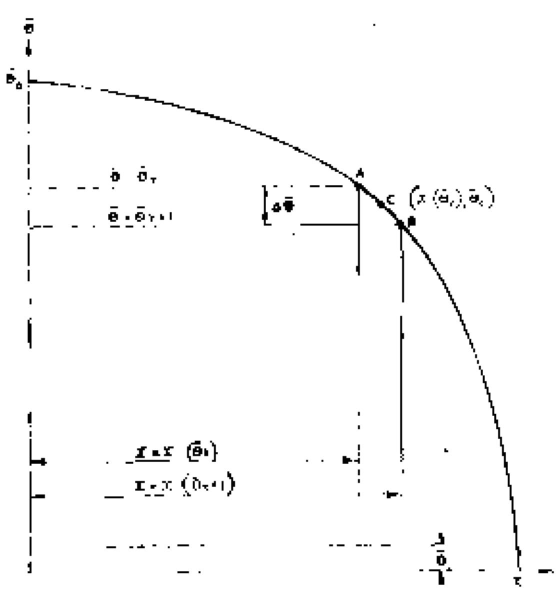

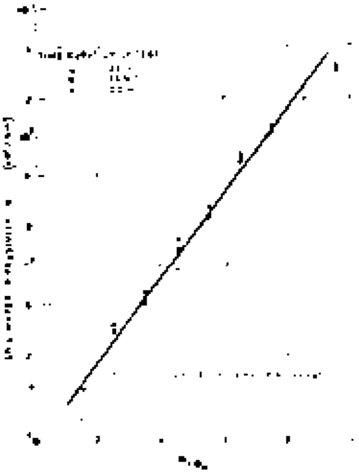

Fig 2. Variation of soil water diffusivity with water content

maximum error introduced in the calculation of $D(\theta)$ by taking C as the point $(x(\theta_{r+1}), t^{\frac{1}{2}}_{r+1})$ will be

$$\pm\left(\frac{x(\theta_{r+1}) - x(\theta_r)}{2t\Delta\theta}\right)\left(\frac{x(\theta_r)\,\Delta\theta}{2}\right) \pm \left(\frac{(x(\theta_{r+1}) - x(\theta_r))x(\theta_r)}{4t}\right)$$

This error will be fairly small except at very small θ values.

It can be seen that because of the iterative nature of the above equation [12] for the calculation of D, the most appropriate method will be to perform the calculations in table form. The calculation procedures are shown in Appendix I.

Fig 2 shows the variation of D with θ as calculated from the three different moisture profiles of identical samples of a kaolinitic soil (identified as English clay) but with different time spans. It can be seen that the relationship between D and θ is practically the same for tests at different time spans. This indicates the viability of the present method of calculation and the theories involved. Furthermore, it should also be noted that there is a very marked linear relationship between log D and θ (or D and e^{θ}), except at the two extreme ends of the moisture content range. It follows that a further fairly simple check on the applicability of the present method of diffusivity calculation is possible by rendering the empirical relationship between D and e^{θ} obtained from Fig 2 into the diffusion equation [3a]. This can then be solved numerically by the finite difference method and compared with actual test results.

Computer solution of diffusion equation

Writing the diffusion equation [3a] in finite difference form

$$(\theta_n^{j+1} - \theta_n^j)/\Delta t = \frac{1}{\Delta x}\left(D(\theta_{n+\frac{1}{2}}^{j})(\theta_{n+1}^{j} - \theta_n^{j})/\Delta x - D(\theta_{n-\frac{1}{2}}^{j})(\theta_n^{j} - \theta_{n-1}^{j})/\Delta x\right) \quad \ldots\ldots[14]$$

where n, j are respectively space and time iterations. Expressing in explicit form and making the approximation that

$$D(\theta_{n+\frac{1}{2}}^{j}) = \tfrac{1}{2}(D(\theta_{n+1}^{j}) + D(\theta_n^{j}))$$

the above equation [14] becomes

$$\theta_n^{j+1} = \frac{\Delta t}{2(\Delta x)^2}\left((D(\theta_{n+1}^{j}) + D(\theta_n^{j}))(\theta_{n+1}^{j} - \theta_n^{j}) - (D(\theta_n^{j}) + D(\theta_{n-1}^{j}))(\theta_n^{j} - \theta_{n-1}^{j})\right) + \theta_n^{j} \quad \ldots\ldots[15]$$

It follows from equation [15] that if both (1) the moisture profile at a certain time $t = j\Delta t$, and (2) the $D(\theta)$ function, are known, then the profile at other time values can be calculated numerically by the computer. For stability requirement of the numerical solution, the Δt and Δx values must be chosen in such a way that

$$\frac{D_{max}\,\Delta t}{(\Delta x)^2} \leq 0{\cdot}5$$

where D_{max} is the maximum diffusivity value which is equal to $D(\theta_0)$ in the present case. The flow diagram for this computer program is shown in Appendix II.

Fig 3 shows the actual test results together with the computer solutions thus obtained at various time durations by using the empirical relation between log D and θ, and the water content distribution at t = 1500min. It can be seen that the comparison between theoretical and actual results is very favourable.

Practical applications

The previous simple procedures proposed in determining the soil water diffusivity-water content relationship and the finite difference equation [15] together with the computer program developed for the above equation, can be readily applied to give an approximate but quick solution to such practical problems as:

(1) the infiltration of rainwater into unsaturated soil in an unprotected natural slope, and

(2) the pre-ponding of unsaturated soil in foundation treatment for potentially collapsing or swelling soils.

In both cases, the initial water content distribution is not uniform, hence a prediction of the subsequent water content distribution is quite difficult. However, for determining the

Fig 3. Actual and predicted water content-distance curves

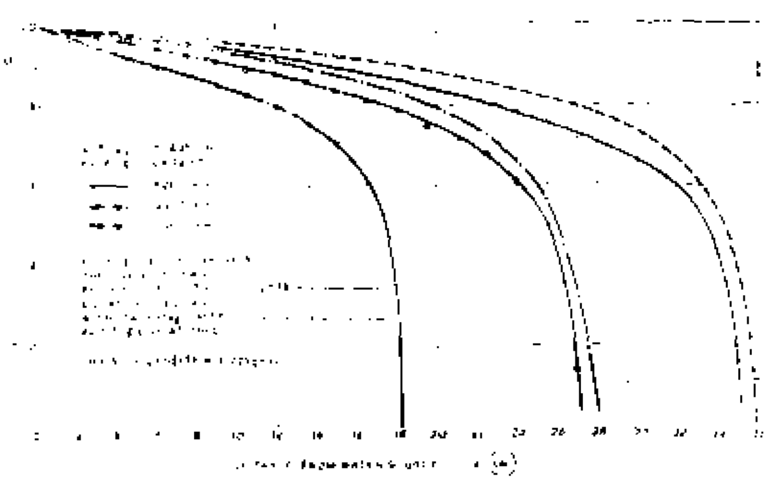

stability of the unprotected natural slope or the subsequent bearing capacity of the pre-ponded foundation, a knowledge of the water content distribution at any instant is essential. This can now be done quite easily as follows:

(1) Conduct some simple horizontal infiltration tests on the type of soil under consideration, with a uniform water content, and determine the water content distribution at the end of each test. An initially air-dried sample will be most convenient and useful.

(2) Calculate the average soil water diffusivity-water content relationship from the water content-distance curves thus determined in (1) by the method proposed in the present paper. (See also Appendix 1 for the sample calculation.)

(3) Measure the initial water content distribution in the site under consideration.

(4) With the boundary condition, initial condition, and soil water diffusivity-water content relationship all known, the water content distribution at any time can be easily determined by a computer solution of the finite difference equation [15]. If necessary, equation [15] can be easily modified to two- or three-dimensional case.

(5) As for a given type of soil, the relationships between water content and soil suction, and hence between soil suction and soil strength, can be determined in the laboratory (7, 8), the soil strength at any point and at any instant can therefore be easily estimated.

With a knowledge of the soil strength distribution at any instant available, it is then possible to predict more competently the stability of an unprotected natural slope under prolonged heavy rainstorm, and to take protective measures as necessary, or to determine the optimum time required for the pre-ponding of a foundation.

Conclusions

The present paper demonstrates how some of the practical civil engineering problems concerning unsaturated soils can be tackled by a combination of the unsaturated flow theories, simple laboratory tests, and numerical analysis with the aid of an electronic digital computer.

Acknowledgement

The research was conducted under a National Research Council grant, Canada (R N Yong, Grantee) at McGill University.

Appendix 1—Sample calculation of soil water diffusivity

A sample calculation is given in Table 1. This is based on the soil water content distribution data in Fig 3 of a kaolinitic soil identified as English clay. The detailed calculation procedures are as follows:

(1) The best-fitted water content (θ) versus distance (x) curve at a certain given time is constructed graphically through the experimental points as can be seen from Fig 3.

(2) Choose the number of equal intervals, n, into which $(\theta_o - \theta_i)$, or θ_o is to be divided. From this $\Delta\theta$ will also be fixed from equation [9]. In the present example, since $\theta_i = 0$, $\theta_o = 1$ (see Fig 3), and n has been chosen to be 10, it follows from equations [9] and [10] respectively that

$$\Delta\theta = 0{\cdot}1$$

$$\theta_r = (10 - r)/10 \qquad \text{..........[10a]}$$

(3) Enter from $r = 9$ to $r = 0$ in column (1) of Table 1, then the θ_r values in column (2) can be entered accordingly by the use of equation [10a].

(4) The corresponding $x(\theta_r)$ values in column (3) can be read from the best-fitted water content (θ) versus distance (x) curve in Fig 3.

(5) $(x(\theta_{r+1}) - x(\theta_r))$ in column (4) can be formed from column (3) by subtraction.

(6) $(x(\theta_{r+1}) - x(\theta_r))/\Delta\theta$ in column (5) can be formed by dividing the corresponding value in column (4) by $\Delta\theta$.

(7) $x(\theta_r)\Delta\theta$ in column (6) can be formed by multiplying the corresponding value in column (3) by $\Delta\theta$.

(8) For the $\int_{\theta_i}^{\theta_{r+1}} x\,d\theta$ values in column (7), the first row is equal to $x(\theta_1)(\theta_{n-1} - \theta_i)$. The second row is equal to the sum

Table 1. Sample calculation of soil water diffusivity

(English clay – dry bulk density = 1·225gm/cc, Duration of test = 6000min.)

1	2	3	4	5	6	7	8
$n-r$	θ_r	$x(\theta_r)$ (cm)	$x(\theta_{r+1}) - x(\theta_r)$	$(x(\theta_{r+1}) - x(\theta_r))/\Delta\theta$	$x(\theta_r)\Delta\theta$	$\int_{\theta_i}^{\theta_{r+1}} x\,d\theta$	$D(\theta_{r+1})$ (cm²/min)
						(1 373)	
1	0·1	35·10			3·510		
			0·15	1·5		4·883	0·00610
2	0·2	34·95			3·495		
			0·20	2·0		8·378	0·00140
3	0·3	34·75			3·475		
			0·50	5·0		11·853	0·00493
4	0·4	34·25			3·425		
			0·70	7·0		15·278	0·00891
5	0·5	33·55			3·355		
			1·80	18·0		18·633	0·02795
6	0·6	31·75			3·175		
			3·90	39·0		21·809	0·07088
7	0·7	27·85			2·785		
			5·35	53·5		24·593	0·10964
8	0·8	22·50			2·250		
			8·70	87·0		26·843	0·19461
9	0·9	13·80			1·380		
			13·80	138·0		28·223	0·32456
10	1·0	0					

of the first row in this column and the first row in column (6); the third equal to the sum of its second row and the second row in column (6); and so on.

(9) The $D(\theta_{i,j})$ values in column (8) are calculated, according to equation (12), by multiplying column (7) and column (5) together, and dividing the product by $2t$. In the present example, the time duration of the test, t, is equal to 1500min.

Appendix II — Flow diagram of computer program

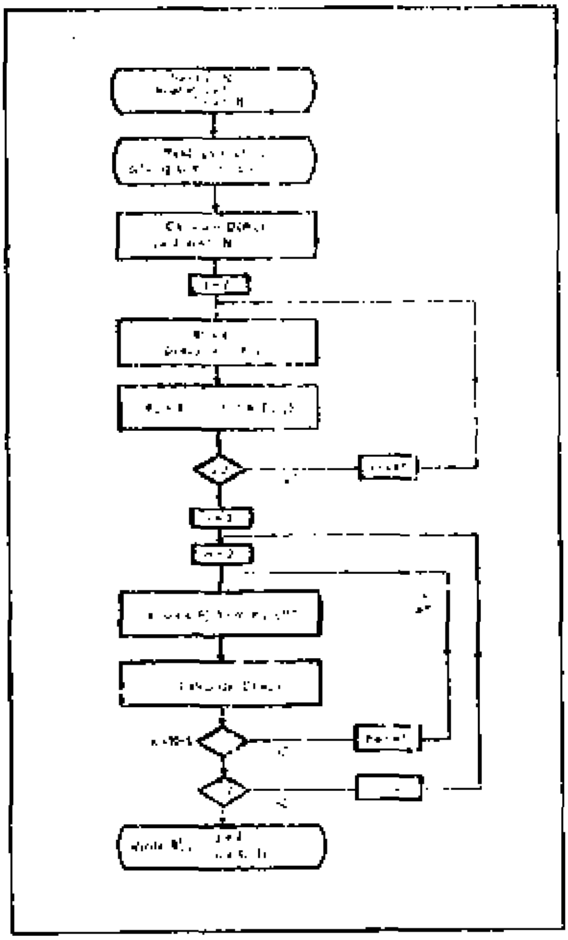

References

1. Gardner, W R, 'Calculation of capillary conductivity from pressure plate outflow data', *Soil Sci Soc Amer Proc*, 1956, 20: 317-320.
2. Miller, E E, and Elrick, D E, 'Dynamic determination of capillary conductivity extended for non-negligible membrane impedance', *Soil Sci Soc Amer Proc*, 1958, 22: 483-486.
3. Kunze, R J, and Kirkham, D, 'Simplified accounting for membrane impedance in capillary conductivity determination', *Soil Sci Soc Amer Proc*, 1962, 26: 421-426.
4. Wong, H Y, and Yong, R N, 'Impedance effects on unsaturated flow in low swelling soil', Amer Soc Civil Engrs, *J Soil Mech Found Div*, 1972, 98: 837-841.
5. Bruce, R R, and Klute, A, 'The measurement of soil moisture diffusivity', *Soil Sci Soc Amer Proc*, 1956, 20: 458-462.
6. Aitchison, G D, Russam, K, and Richards, B G, 'Engineering concepts of moisture equilibria and moisture changes in soils', Ministry of Transport, RRL Report LR38, Crowthorne, 1965 (Road Research Laboratory).
7. Dumbleton, M J, and West, G, 'The suction and strength of remoulded soils as affected by composition', Ministry of Transport, RRL Report LR 306, Crowthorne, 1970 (Road Research Laboratory).
8. Yong, R N, Japp, R D, and How, G, 'Shear strength of partially saturated clays', 4th Asian Regional Conference on Soil Mechanics and Foundation Engineering, Thailand, 1971, 1: 183-187.

Journal, Soil Mechanics and Foundations Division, Proc., American Society of Civil Engineers, V98:SM8, August 1972.

IMPEDANCE EFFECTS ON UNSATURATED FLOW IN A NONSWELLING SOIL

By Hong-Yau Wong[1] and Raymond N. Yong,[2] M. ASCE

INTRODUCTION

In laboratory studies of unsaturated flow in soils, contact between the unsaturated test specimen and available water is through a saturated porous plate (Fig. 1). Ideal conditions are established when the permeability of the porous plate is extremely large in comparison with the effective permeability of the test specimen. However, because specimen permeability is seldom established a priori, the permeability of the porous plate, K_p, is frequently near to, or smaller than, that of the specimen, K_s. Thus, initial or plate impedance could arise which in turn could produce anomalous test results.

The purpose of this study is to provide a means for predicting the impedance effect on infiltration through capillary flow analysis, and to explain thereby (from laboratory testing) the concavity observed in the wetting front distance $x - t^{1/2}$ relationship.

THEORY

In unsaturated fluid flow through nonswelling soils, the movement of water is described by an equation derived from the Darcy equation and the equation of continuity. Where the proper experimental constraints are applied, it is seen that the relationship between x and $t^{1/2}$ is linear; in which x = wetting front distance from porous plate; and t = time. With the introduction of a plate impedance at the water inlet, problems arise as follows.

First, the plate itself is just equivalent to a layer of unsaturated soil having a permeability value different from that of the sample. Therefore, water will be flowing through a layered soil system. The thicker the plate, and the lower its permeability value, the larger will be its effect on the flow, especially during the initial stage.

Secondly, the amount of time that has elapsed before the plane $x = 0$ can attain full saturation will increase with the increase in plate impedance. The larger the time lag, the more the flow will be affected.

To account for the first effect, a simple analysis is employed, using the equation which governs the horizontal capillary flow in granular soil as de-

Note.—This paper is part of the copyrighted Journal of the Soil Mechanics and Foundations Division, Proceedings of the American Society of Civil Engineers, Vol. 98, No. SM8, August, 1972. Manuscript was submitted for review for possible publication on February 22, 1972.

[1] Research Engr., The Cementation Research Company Limited, Rickmansworth, Herts, England.

[2] Prof., Dept. of Civ. Engrg. and Applied Mechanics, McGill Univ., Montreal, Canada.

rived by Taylor (1). This equation is

$$Sn\,\frac{dx}{dt} = K_s\,\frac{h_o + h_c^*}{x} \qquad (1)$$

in which K_s = capillary permeability; n = porosity of the sample; S = capillary degree of saturation; h_c^* = effective capillary head; h_o = applied hydrostatic head; and x is measured from the interface between the porous plate and the soil sample. The use of the preceding equation to a low swelling clay soil is

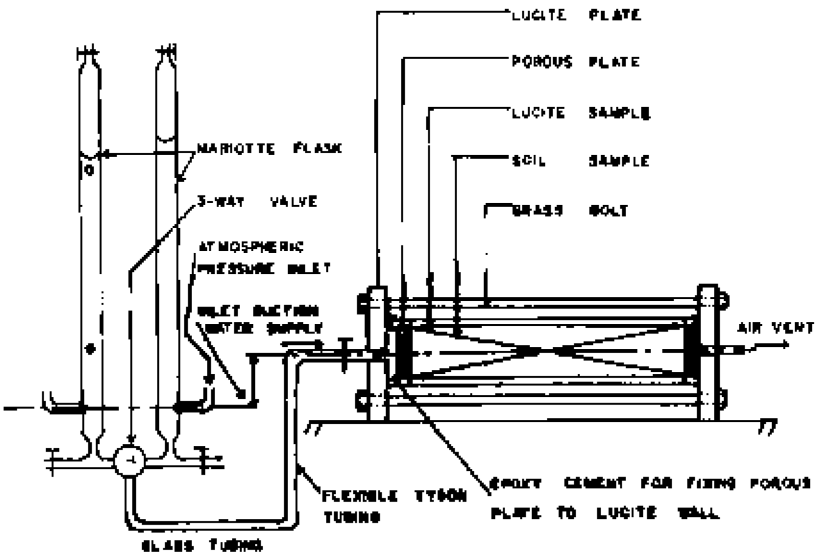

FIG. 1.—SCHEMATIC REPRESENTATION OF EXPERIMENTATION

justified because the average degree of saturation is practically time independent.

Let the plate have a thickness L, permeability K_p, and the same cross-sectional areas as that of the sample. At time t, the wetting front has advanced a distance X, then the effective permeability $\overline{K}$ of the system will be given by

$$\overline{K} = \frac{X + L}{\dfrac{L}{K_p} + \dfrac{X}{K_s}} \qquad (2)$$

and the effective hydraulic gradient $= \dfrac{h}{X + L}$ (3)

in which $h = h_o + h_c^*$.

Substituting Eqs. 2 and 3 into Eq. 1 and solving the resultant ordinary differential equation, subject to the initial condition, $t = 0$; $x = 0$ gives

$$X = \left[\left(\frac{LK_s}{K_p}\right)^2 + \frac{2hK_s}{Sn}\,t\right]^{1/2} - \frac{LK_s}{K_p} \qquad (4)$$

The simple analysis shows that if $K_p >> K_s$ or t is large, the term $2LK_s X/K_p$ will be negligible, and X will thus vary linearly with the square root of time.

To examine the second effect of plate impedance, it is assumed that a time, Δt, for the plane $x = 0$ to attain the saturated water content is needed. During this time interval Δt, the water content, θ, at the plane $x = 0$ increases linearly with time. For convenience, the variable θ is changed to $\bar{\theta}$ by putting $\bar{\theta} = \theta/\theta_o$, in which θ = the volumetric moisture content; and θ_o = the saturated volumetric moisture content. At any time $t < \Delta t$, $\bar{\theta}$ at $x = 0$ is given by $\int_0^t (\partial\bar{\theta}/\partial t)\, dt$. At time $t = \Delta t$, $\bar{\theta}$ at $x = 0$ is given by $\int_0^t (\partial\bar{\theta}/\partial t)\, dt = 1$. As $\Delta t \rightarrow 0$, $\partial\bar{\theta}/\partial t = \delta(t)$, the Dirac function.

It follows that the initial and boundary conditions for the classical diffusion equation:

$$\frac{\partial\bar{\theta}}{\partial t} = \frac{\partial}{\partial x}\left[D(\theta)\,\frac{\partial\bar{\theta}}{\partial x}\right] \qquad (5)$$

should be rewritten as

$$t = 0;\ x = 0:\ \bar{\theta} = \frac{\theta_i}{\theta_o} \qquad (6)$$

$$t > 0;\ x = 0:\ \bar{\theta} = [1 - H(t - \Delta t)] \int_0^t \frac{\partial\bar{\theta}}{\partial t}\, dt + H(t - \Delta t) \qquad (7a)$$

in which $H(t - \Delta t) = 0 \quad t < \Delta t$
$\qquad\qquad\qquad = 1 \quad t \geq \Delta t$ (7b)

As the unsaturated permeability and thus, the rate of wetting front advance will increase with the increase in water content at the plane $x = 0$, the curve of x versus $t^{1/2}$ will therefore concave upward until $t = \Delta t$, following which it should remain sensibly linear.

It can be seen theoretically that the preceding two effects tend to give the x versus $t^{1/2}$ curve a curvilinear portion concaving upward at small values of time.

EXPERIMENTATION

The essence of the present experimentation consisted of a series of three basic kinds of tests in which water was allowed to flow into a semi-infinite, cylindrical, air-dried soil sample under zero hydrostatic head, and subject to the initial and boundary conditions as given in Eqs. 6 and 7a. In each test, the plate impedance was varied while the same type of soil sample was used.

The porous plate used was a sand cement mixture of 1-3/8 in. diam and thickness 0.3 in. In order to prepare porous plates of various impedance, different proportions of sand, cement and water were used. These were air-dried, and then saturated with de-aired and distilled water.

ANALYSIS

The typical experimental tests shown in Fig. 2 using plates of various impedance values indicate that the x versus $t^{1/2}$ curve is initially curvilinear,

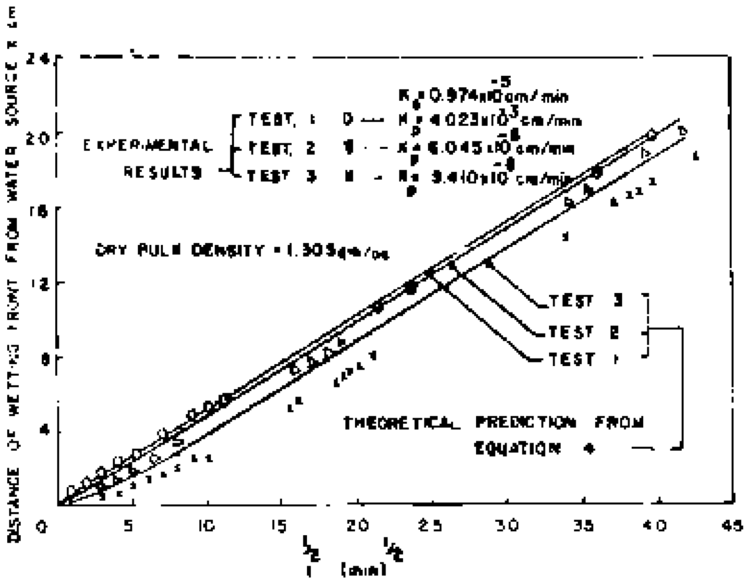

FIG. 2.—RELATIONSHIP BETWEEN DISTANCE OF WETTING FRONT FROM WATER SOURCE AND SQUARE ROOT OF TIME

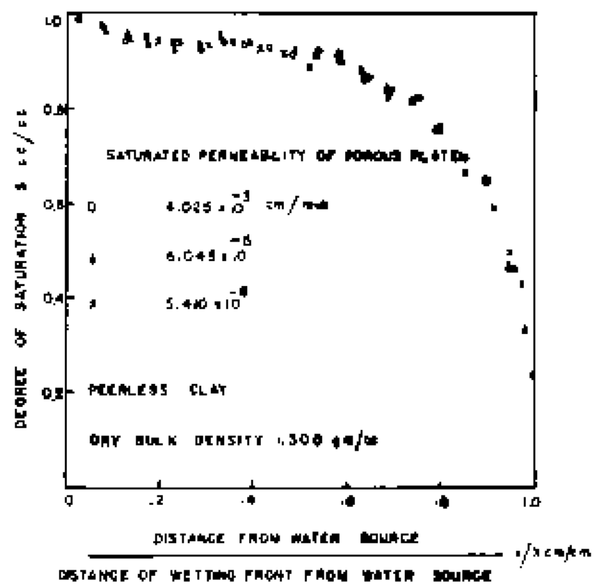

FIG. 3.—RELATIONSHIP BETWEEN DEGREE OF SATURATION AND RATIO OF DISTANCES FROM WATER SOURCE

concaving upward at small time values. This is in good agreement with the previously developed theoretical considerations. A comparison of permeability values of the various porous plates with that of the Peerless clay shows that the effect of plate impedance is quite appreciable even for a permeability value of the plate of about the same order of magnitude as that of the saturated clay. The results show that when the permeability value of the plate is about 100 times larger than that of the sample, it then becomes negligible and the x versus $t^{1/2}$ curve will be a straight line passing through the origin.

Furthermore, the solid curves in Fig. 2 represent the theoretical prediction from Eq. 4, using the various ratios of K_s/K_p given. These are slightly above the experimental points, with the exception of test 1. Bearing in mind that Eq. 4 only takes into account the first effect, the preceding prediction seems to be in the right order.

It is shown that on the other hand, from a comparison of the soil moisture profiles in Fig. 3 that the present range of plate impedance values has practically no effect on the shape of the profiles.

CONCLUSION

In the method developed for examination of plate impedance effects on infiltration into nonswelling soils, it is shown that when $K_p >> K_s$, the impedance effect is negligible. However, when $K_p \approx K_s$, initial concavity is both predicted and observed in the $x - t^{1/2}$ relationship. It is further shown from experimentation that while plate impedance effects are observed in time-rate of infiltration, the moisture profiles remain sensibly unaffected.

It follows that in order to obtain a reliable estimate of the rate of soil wetting in practice, either a plate with permeability value at least 100 times larger than that of the sample should be used, or the testing times should be increased so as to obtain (and include) a sufficiently large linear portion of the $x - t^{1/2}$ relationship.

ACKNOWLEDGMENT

This study was conducted in the Soil Mechanics Laboratory of McGill University with financial assistance and support provided by the National Research Council of Canada.

APPENDIX.—REFERENCE

1. Taylor, D. W., *Fundamentals of Soil Mechanics*, John Wiley and Sons, Inc., New York, N.Y., 1948.